Prepared in cooperation with the Lahontan Regional Water Quality Control Board

# Survey of Chromium and Selected Element Concentrations in Rock, Alluvium, and Core Material

Chapter B of

**Natural and Anthropogenic (Human-Made) Hexavalent Chromium, Cr(VI), in Groundwater near a Mapped Plume, Hinkley, California**

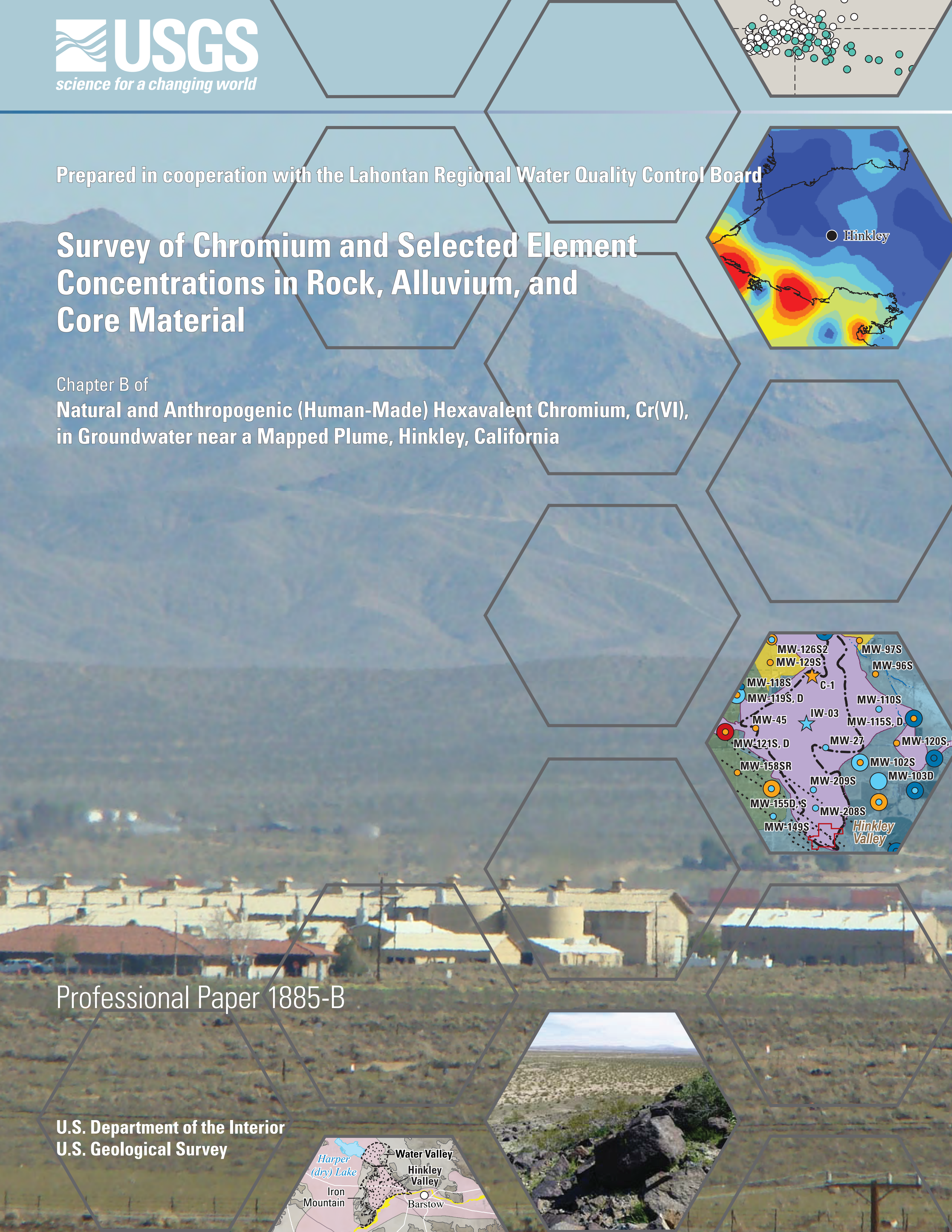

Professional Paper 1885-B

U.S. Department of the Interior
U.S. Geological Survey

**Front cover**

First and second principal component scores for surficial alluvium

Chromium concentrations in soil near Hinkley, California.

Background photograph: Pacific Gas and Electric Company (PG&E) compressor station, Hinkley, California, March 2009. Photograph by Steven Perry, ARCADIS, Inc., courtesy of PG&E.

Chromium concentrations in aquifer material, Hinkley and WaterValleys, western Mojave Desert, California.

Hornblende diorite, Iron Mountain, Hinkley Valley, western Mojave Desert, California

Location of study area and surrounding features

# Survey of Chromium and Selected Element Concentrations in Rock, Alluvium, and Core Material

Chapter B of

## Natural and Anthropogenic (Human-Made) Hexavalent Chromium, Cr(VI), in Groundwater near a Mapped Plume, Hinkley, California

By John A. Izbicki and Krishangi D. Groover

Prepared in cooperation with the Lahontan Regional Water Quality Control Board

Professional Paper 1885-B

**U.S. Department of the Interior**
**U.S. Geological Survey**

U.S. Geological Survey, Reston, Virginia: 2023

Suggested citation:
Izbicki, J.A., and Groover, K.D., 2023, Survey of chromium and selected element concentrations in rock, alluvium, and core material, Chapter B of Natural and anthropogenic (human-made) hexavalent chromium, Cr(VI), in groundwater near a mapped plume, Hinkley, California: U.S. Geological Survey Professional Paper 1885-B, 37 p., https://doi.org/10.3133/pp1885B.

Associated data for this publication:
Groover, K.D., and Izbicki, J.A., 2018, Field portable X-ray fluorescence and associated quality control data for the western Mojave Desert, San Bernardino County, California: U.S. Geological Survey data release, https://doi.org/10.5066/P9CU0EH3.

Morrison, J.M., Benzel, W.M., Holm-Denoma, C.S., and Bala, S., 2018, Grain size, mineralogic, and trace-element data from field samples near Hinkley, California: U.S. Geological Survey data release, https://doi.org/10.5066/P9HUPMG0.

ISSN 2330-7102 (online)

# Acknowledgments

This study was developed by the U.S. Geological Survey (USGS) with input from a technical working group (TWG) composed of community members, the Lahontan Regional Water Quality Control Board (RWQCB), the Independent Review Panel Manager (Project Navigator, Ltd.), Pacific Gas and Electric Company (PG&E), and consultants for PG&E. The study was funded cooperatively under an agreement between the Lahontan RWQCB and the USGS. Funding for the study was provided by PG&E to the Lahontan RWQCB. Logistical support for field work, including access to wells, was provided by PG&E. The TWG met approximately quarterly during the study to provide input to the study, and the Hinkley community was updated annually on study progress.

The authors thank the many people involved in the design and implementation of this study including the staff of the Lahontan RWQCB, the staff of PG&E and their consultants, and the staff of Project Navigator, Ltd. The authors also acknowledge and thank the many involved community members who allowed access to their properties for sample collection, and who collectively donated thousands of hours on behalf of the local community in support of this project and for resolution of other issues related to anthropogenic hexavalent chromium, Cr(VI), within the Hinkley area.

# Contents

## Figures

## Tables

# Conversion Factors

U.S. customary units to International System of Units

| Multiply | By | To obtain |
|---|---|---|
| | Length | |
| foot (ft) | 0.3048 | meter (m) |
| mile (mi) | 1.609 | kilometer (km) |
| | Area | |
| square mile ($mi^2$) | 259.0 | hectare (ha) |
| square mile ($mi^2$) | 2.590 | square kilometer ($km^2$) |
| | Flow rate | |
| cubic foot per second ($ft^3/s$) | 0.02832 | cubic meter per second ($m^3/s$) |

International System of Units to U.S. customary units

| Multiply | By | To obtain |
|---|---|---|
| | Length | |
| centimeter (cm) | 0.3937 | inch (in.) |
| millimeter (mm) | 0.03937 | inch (in.) |
| | Mass | |
| milligram (g) | 0.00003527 | ounce, avoirdupois (oz) |
| kilogram (kg) | 2.205 | pound avoirdupois (lb) |

Temperature in degrees Celsius (°C) may be converted to degrees Fahrenheit (°F) as follows:

$$°F = (1.8 \times °C) + 32.$$

## Datum

Vertical coordinate information is referenced to the North American Vertical Datum of 1988 (NAVD 88).

Horizontal coordinate information is referenced to the North American Datum of 1983 (NAD 83).

Below land surface (bls) is the datum used to describe depth.

Altitude, as used in this report, refers to distance above the vertical datum.

## Supplemental Information

Concentrations of chemical constituents in water are given in either milligrams per liter (mg/L) or micrograms per liter (µg/L).

Concentrations of chemical constituents in solids are given in milligrams per kilogram (mg/kg).

Concentrations of chemical constituents in rock or unconsolidated solids are given in milligrams per kilogram (mg/kg).

Redox, a combination of the words reduction and oxidation, refers to chemical processes in which one substance or molecule gains an electron (is reduced and its oxidation state is decreased) and another loses an electron (is oxidized and its oxidation state is increased). The processes of oxidation and reduction occur simultaneously and cannot occur independently.

## Abbreviations

| | |
|---|---|
| Cr(III) | trivalent chromium having an oxidation state of +3 |
| Cr(VI) | hexavalent chromium having an oxidation state of +6 |
| ICP-MS | inductively coupled plasma-mass spectrometry |
| MCL | maximum contaminant level |
| MSE | mean squared error |
| PCA | principal component analysis |
| PG&E | Pacific Gas and Electric Company |
| pXRF | portable (handheld) X-ray fluorescence |
| $R^2$ | coefficient of determination |
| SRL | study reporting level |
| SSA | summative-scale analysis |
| USGS | U.S. Geological Survey |
| WDXRF | wave-length dispersive X-ray fluorescence |

# Survey of Chromium and Selected Element Concentrations in Rock, Alluvium, and Core Material

By John A. Izbicki and Krishangi D. Groover

## Abstract

Between 1952 and 1964, hexavalent chromium, Cr(VI), was released into groundwater from the Pacific Gas and Electric Company (PG&E) compressor station in Hinkley, California, in the western Mojave Desert 80 miles northeast of Los Angeles, California. In 2015, the extent of anthropogenic Cr(VI) in groundwater in Hinkley and Water Valleys was uncertain, and some Cr(VI) in groundwater may be naturally occurring from rock and aquifer material.

On the basis of more than 1,500 portable (handheld) X-ray fluorescence (pXRF) measurements on more than 250 samples of rock, surficial alluvium, and core material from selected wells in Hinkley and Water Valleys, chromium concentrations are commonly low compared to the average bulk continental abundance of 185 milligrams per kilogram (mg/kg). However, chromium concentrations are as high as 530 mg/kg in mafic hornblende diorite that crops out along the western margin of Hinkley Valley in Iron Mountain. Other chromium-containing rocks in the area are either (1) not consistently high in chromium, (2) have limited areal extent, or (3) in the case of basalt, are present only in Water Valley.

Chromium concentrations in core material adjacent to the screened intervals of wells sampled for water chemistry and isotopic composition as part of the U.S. Geological Survey Cr(VI) background study ranged from less than the study reporting level (SRL) of 5 mg/kg to 410 mg/kg, with a median concentration of 23 mg/kg. Chromium concentrations in core material were lower in the eastern subarea and higher in the western and the northern subareas of Hinkley Valley and in Water Valley. The highest chromium concentration in core material was in weathered hornblende diorite bedrock. Chromium concentrations in core material adjacent to the screened interval of sampled wells were log-normally distributed below a threshold of 85 mg/kg, and 3 percent of chromium concentrations were greater than 85 mg/kg. Manganese can oxidize trivalent chromium, Cr(III), to Cr(VI). Similar to chromium, manganese concentrations in core material also were log-normally distributed below a threshold of 970 mg/kg, and 5 percent of manganese concentrations were greater than 970 mg/kg. Both chromium and manganese concentrations were higher in fine-textured core material and in visually abundant iron- and manganese-oxide coatings on the surfaces of mineral grains. High concentrations of chromium and manganese in core material commonly co-occurred. Fine-textured core material, chromium concentrations greater than 85 mg/kg, and manganese concentrations greater than 970 mg/kg in core material adjacent to the screened interval of sampled wells were selected for use as metrics (threshold values) within a summative-scale analysis (SSA) developed to identify natural and anthropogenic Cr(VI) in water from wells later within this professional paper (chapter G).

Principal component analysis (PCA) of 18 elements within surficial alluvium, rock, and core material measured using pXRF shows distinct elemental assemblages associated with (1) older and more recent “Mojave-type” deposits, including alluvium and lake-margin (beach) deposits sourced from the Mojave River, (2) alluvium eroded from mafic rock, including hornblende diorite that crops out on Iron Mountain, (3) alluvium eroded from felsic volcanic and hydrothermal rock that crops out on Mount General along the eastern margin of Hinkley Valley, (4) playa/mudflat and other fine-textured deposits, and (5) material with visually abundant iron- and manganese-oxide coatings. Most wells sampled as part of this study were completed in Mojave-type deposits. Portable (handheld) X-ray fluorescence data measured on core material from those wells do not appear to be different or unusual compared to the magnitude and range of data from the larger Mojave River groundwater basin, and the core material has a low-chromium, felsic composition consistent with a Mojave River origin. In general, the elemental composition of core material from wells was not measurably altered by admixtures with local mafic, felsic volcanic, or hydrothermal source materials; although, where present, admixtures with basalt may contribute chromium to core material.

## B.1. Introduction

The U.S. Geological Survey was requested by the Lahontan Regional Water Quality Control Board to complete an updated background study of hexavalent chromium, Cr(VI), concentrations in Hinkley and Water Valleys. Chromium occurs naturally in rocks, alluvium, and soils and is the 21st most abundant element in the Earth's crust (Emsley, 2001). The average chromium concentration in the bulk continental crust is estimated to be 185 milligrams per kilogram (mg/kg; Nriagu and Nieboer, 1988; Reimann and de Caritat, 1998). Chromium concentrations are higher in basaltic and ultramafic rocks, which have average concentrations of about 250 and 2,300 mg/kg, respectively (Reimann and de Caritat, 1998), than in granitic rocks, which have an average concentration of about 10 mg/kg (Reimann and de Caritat, 1998).

Geochemical surveys of rock, soil, and stream sediments reveal patterns in the natural distribution of trace elements that are related to geologic source materials and processes that alter the composition of those materials (Graham, and others, 2015). Data from these surveys are important for mineral exploration, risk-based assessment of contaminated land, environmental regulation, human and animal health, agriculture, land-use planning, and water quality. Numerous regional, national, and international-scale surveys describing elemental distributions within the near-surface environment have been completed (Shacklette and others, 1971; Shacklette and Boerngen, 1984; Gough and others, 1988, 2005; U.S. Geological Survey, 2004; Smith and others, 2014; Graham and others, 2015). Chromium-containing rock, abundant elsewhere in California (Kruckeberg, 1984), is not mapped in the Hinkley area (fig. B.1*A*), and the most recent national-scale survey of the elemental composition of soils within the United States (Smith and others, 2014) showed regional chromium concentrations in the western Mojave Desert were low, with chromium concentrations in the Hinkley area commonly less than 10 mg/kg (fig. B.1*B*). Similar results were obtained for rock and surficial alluvium from a regional-scale study by Groover and Izbicki (2019), although they identified areas within the Mojave River groundwater basin (fig. B.1) that have locally higher chromium concentrations.

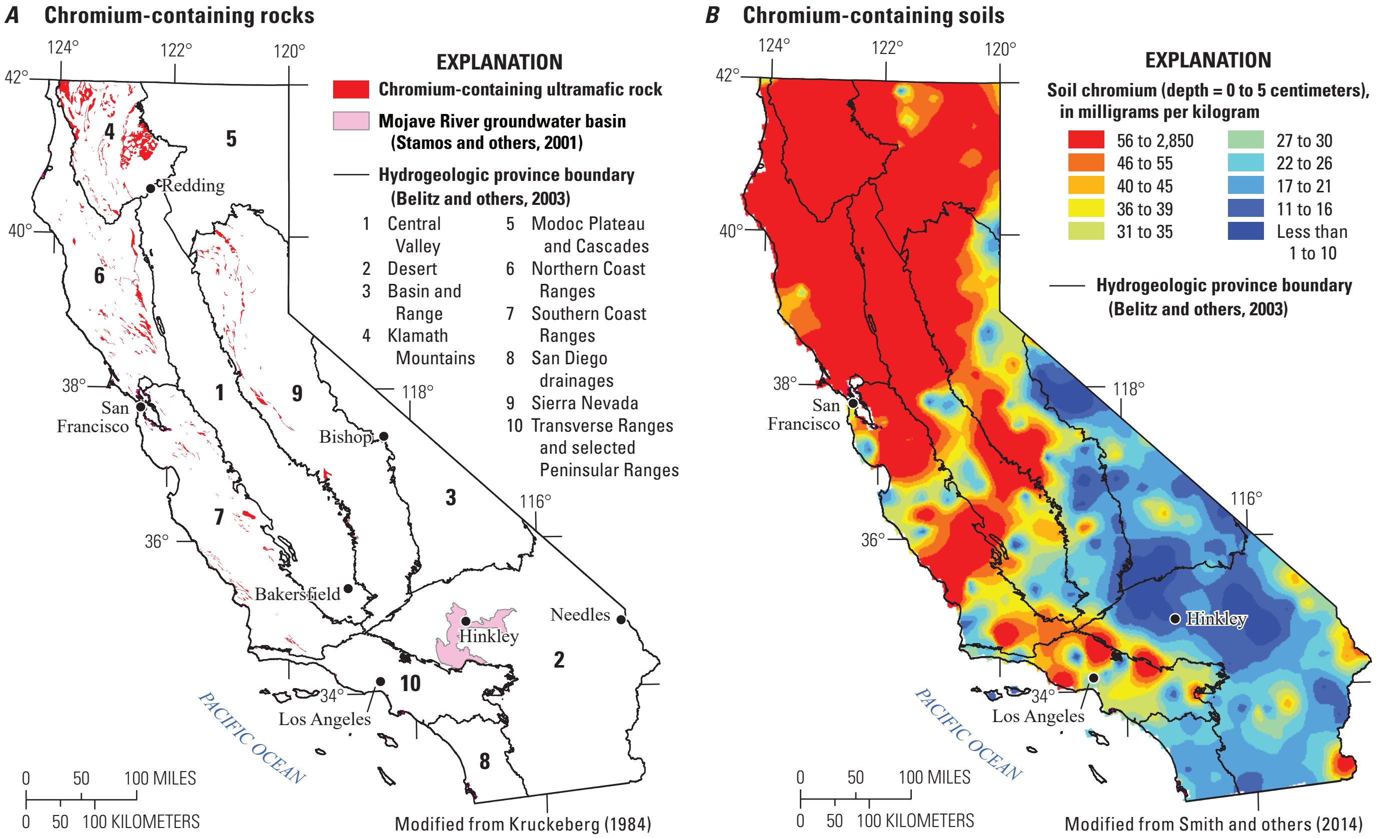

Base from U.S. Geological Survey and other Federal and State digital data, various scales; Albers Equal-Area Conic projection, standard parallels are 29°30' N. and 45°30' N.; North American Datum of 1983

Base from U.S. Geological Survey and other Federal and State digital data, various scales; Albers Equal-Area Conic projection, standard parallels are 29°30' N. and 45°30' N.; North American Datum of 1983

**Figure B.1.** *A*, Chromium-containing rocks and *B*, chromium concentrations in soils in California.

The purpose of this chapter is to evaluate the distribution of chromium in rock, alluvium, and core material from wells and to identify potential sources of chromium within Hinkley and Water Valleys. Scope of this work included measurement and interpretation of chromium and other selected trace-element concentrations in geologic material using portable (handheld) X-ray fluorescence (pXRF; Groover, 2016; Groover and Izbicki, 2018). Portable (handheld) X-ray fluorescence data are easily and inexpensively collected but are generally considered to be less accurate than other techniques used to measure elemental concentrations in geologic materials. Spatially distributed pXRF data provide context for more quantitative (and expensive) inductively coupled plasma-mass spectrometry (ICP-MS), mineralogy, particle-size and density separates, and sequential-extraction data from selected materials discussed in chapter C within this professional paper.

## B.2. Site Description

The study area is within the 2,120 square mile ($mi^2$) Mojave River drainage in the western Mojave Desert, about 80 miles (mi) northeast of Los Angeles, California. The Mojave River is a geologically recent feature that has its source in the San Bernardino Mountains near Cajon Pass. Cajon Pass was created by movement along the San Andreas Fault over the past 1 to 3 million years. This movement transported chromium-containing mafic rocks within the San Gabriel Mountains to the northwest (Meisling and Weldon, 1989; Cox and others, 2003) and changed the source area contributing alluvium to the Mojave River (Cox and others, 2003; Izbicki and others, 2008; Groover and Izbicki, 2019). As a consequence, older Mojave River deposits, eroded at a time when the San Gabriel Mountains contributed a larger proportion of alluvium directly to the ancestral Mojave River (chapter A, fig. A.5), contain more mafic material and thus have a higher fraction of chromium-bearing minerals and higher chromium concentrations than more recent Mojave River deposits (Groover and Izbicki, 2019).

Hinkley Valley is about 62 $mi^2$ (fig. B.2). Bedrock in Hinkley Valley consists of felsic plutonic (granite) and related intrusive plutons, sheets, and dikes (Dibblee, 1960a, b; Boettcher, 1990; Fletcher and others, 1995; Fletcher and others, 2002). Exposures of mafic plutonic (diorite and gabbro) rock are present in Iron Mountain and near the southern end of Mount General. Unconsolidated deposits overlying bedrock occupy 36 $mi^2$ within Hinkley Valley and include Mojave River stream, lake margin, lake, mudflat/playa, groundwater-discharge deposits, and locally derived alluvial material (chapter A, table A.1; Miller and others, 2018, 2020). Aquifers of interest in Hinkley Valley are composed primarily of unconsolidated deposits consisting of alluvium and near-shore, shallow lake deposits sourced from the Mojave River, referred to as “Mojave-type” deposits for the purposes of this professional paper. Locally derived alluvium, lake deposits, and weathered bedrock are important aquifers or confining units in some areas. The depositional history of unconsolidated deposits within Hinkley and Water Valleys is described in chapter A within this professional paper and in Miller and others (2018, 2020).

On the basis of differences in geology and hydrology, Hinkley Valley was divided into eastern, western, and northern subareas (Izbicki and Groover, 2016, 2018; fig. B.2). The eastern subarea is closest to recharge areas along the Mojave River. Mojave-type deposits in this area are generally less than 160 feet (ft) thick and compose the upper aquifer (ARCADIS and CH2M Hill, 2011). These deposits overlie fine-textured lake deposits, generally described as “blue clay” in geologists and drillers logs (chapter A, fig. A.6). Where present, the blue clay separates unconsolidated deposits into upper and lower aquifers. Fine-textured overbank deposits sourced from the Mojave River, generally described as “brown clay” (chapter A, fig. A.6), are interspersed throughout the upper aquifer and in places separate the upper aquifer into shallow and deep zones (ARCADIS and CH2M Hill, 2011). Mudflat/playa deposits are present at land surface near Mount General and at depth within the eastern subarea. The western subarea consists of Mojave-type deposits overlying groundwater-discharge deposits and weathered bedrock (CH2M Hill, 2013; Miller and others, 2018, 2020). The northern subarea consists of Mojave River alluvium and near-shore lake deposits overlying fine-textured lake and mudflat/playa deposits sourced from the Mojave River and local materials (Stantec, 2013; Miller and others, 2018, 2020). Aquifers within Water Valley consist of lake-margin deposits sourced from the ancestral Mojave River along the margins of Harper (dry) Lake that overlie and interfinger with locally derived alluvium eroded from a number of sources including local basaltic rock and Miocene deposits in the Mud Hills east of the study area (fig. B.2; Miller and others, 2018, 2020).

The Hinkley compressor station is within the eastern subarea of Hinkley Valley. In the fourth quarter of 2015 (October–December; Q4 2015), the regulatory Cr(VI) plume extended about 3.0 mi downgradient from the Hinkley compressor station (fig. B.2; ARCADIS, 2016). Most of the Q4 2015 regulatory Cr(VI) plume was within the eastern subarea of Hinkley Valley and the highest Cr(VI) concentrations in groundwater within the regulatory Cr(VI) plume remained less than 3,000 ft downgradient from the release location within the Hinkley compressor station. However, groundwater having Cr(VI) concentrations greater than the interim regulatory background value of 3.1 micrograms per liter (µg/L; CH2M Hill, 2007; Lahontan Regional Water Quality Control Board, 2008) was present more than 8 mi downgradient and extended into Water Valley (fig. B.2; ARCADIS, 2016).

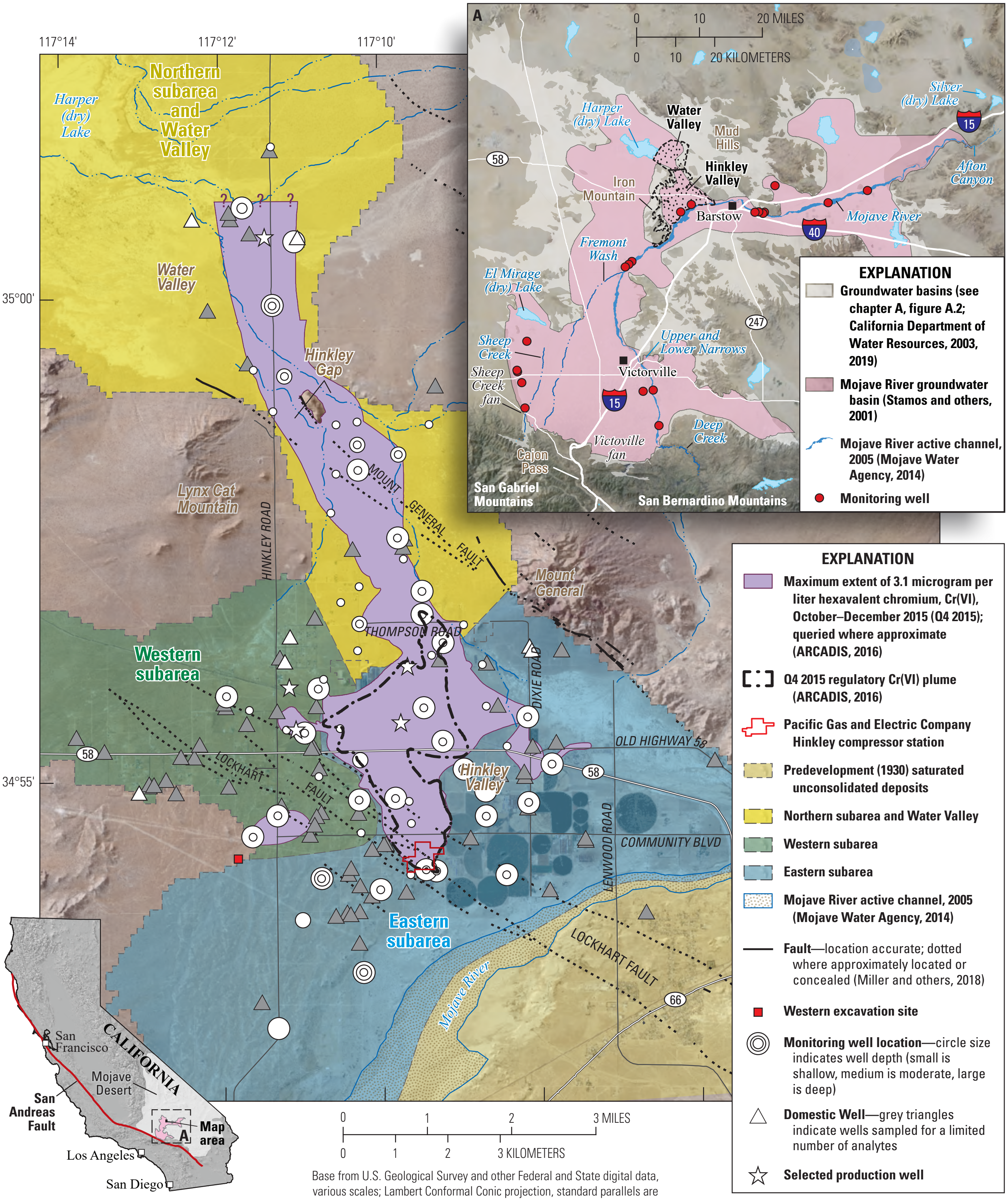

Base from U.S. Geological Survey and other Federal and State digital data, various scales; Lambert Conformal Conic projection, standard parallels are 34.0333° N. and 35.4667° N.; North American Datum of 1983

**Figure B.2.** Location of the Hinkley hexavalent chromium, Cr(VI), background study, western Mojave Desert, California.

Monitoring wells installed for regulatory purposes by Pacific Gas and Electric Company (PG&E) are most commonly identified by the prefix MW, with sites numbered sequentially in the order they were drilled (ARCADIS, 2016). Shallow wells at a site, commonly screened across or just below the water table, are identified with the suffix S, or S1; older monitoring wells are identified with the suffix A. Deeper wells are identified with the suffix D, D1, or D2, or with S2 or S3 if a hydrologically important clay layer is not present between the wells; older monitoring wells are identified with the suffix B (ARCADIS, 2016). The suffix C is used for wells completed in consolidated rock and the suffix R is added if the well is a replacement for a well that was destroyed (ARCADIS, 2016). For the purposes of this professional paper, wells installed by PG&E as part of the U.S. Geological Survey (USGS) Cr(VI) background study are identified with the prefix BG; these sites are numbered sequentially in the order they were permitted, and the BG wells are identified from shallowest to deepest with the suffixes A, B, or C. Although drilling methods changed over time and in response to site conditions and regulatory requirements, most monitoring wells were drilled with auger rigs. Core material, archived by PG&E, was available for most wells installed after 2011 from near the water table to below the depth of the deepest well.

# B.3. Methods

## B.3.1. Field and Laboratory Methods

More than 1,500 pXRF measurements were made on more than 250 samples of surficial alluvium, rock, and core material from selected monitoring wells drilled by PG&E (Groover and Izbicki, 2018; fig. B.3). Samples were collected, handled, and measured using techniques described by Groover and Izbicki (2019). A description of those techniques, including a discussion of quality assurance data for pXRF measurements, follows.

Surficial alluvium was collected from small stream channels draining distinct geologic source terrains within Hinkley and Water Valleys and from the active channel of the Mojave River within Hinkley Valley. Surficial alluvium consisted of silt, sand, and gravel that generally had not been extensively altered by soil-forming processes. Rocks were collected from outcrops in Hinkley and Water Valleys. Sample preparation for surficial alluvium consisted of manually removing organic debris and cobbles and either air-drying or oven-drying at 80 degrees Celsius (˚C). Samples were disaggregated and placed in a sample cup prior to measurement. Sample preparation for rocks consisted of rinsing a freshly exposed surface with tap water and allowing the sample to air-dry prior to measurement. Most samples of surficial alluvium and rock were taken to the USGS office in San Diego for analyses.

Core material collected during monitoring well drilling was available from PG&E archives. In addition to coarse-textured sand and gravel, core material included finer-textured silt and clay materials, many of which had been altered by soil forming and hydrogeologic processes. The presence of visually abundant iron-oxide (reddish) or manganese-oxide (black or dark) coatings on the surfaces of mineral grains was recorded prior to pXRF measurement (Groover and Izbicki, 2018). Core material from at least three depths within the screened interval of 79 wells of the more than 100 wells sampled for water chemistry (chapter E) and isotope composition (chapter F) as part of this study (fig. B.2; more simply referred to as sampled wells) was measured by pXRF. For some wells having complex lithology or unusual features, such as visually abundant oxide coatings, as many as 10 measurements were made within the screened interval of the well. Selected core material from unscreened intervals within sampled wells and from wells not sampled as part of this study also was measured. Limited sample preparation for core material was required, and most measurements were made onsite in the PG&E core storage facility.

Prior to pXRF measurement, rock samples were identified by type, and physical attributes including color and texture were described for surficial alluvium and core material. Color was described using numerical designations according to Munsell soil color charts (Munsell Color, 1975, 1994). Texture was described visually and tactilely using methods developed by Folk (1954), and descriptions follow the National Research Council (1947) classification. Provenance of core materials was described by Miller and others (2018, 2020). Descriptions for rock, surficial alluvium, and core-material samples are available in Groover and Izbicki (2018).

Portable (handheld) X-ray fluorescence measurements were made using an energy-dispersive DP-4000 Delta Premium X-ray fluorescence analyzer (Olympus, Waltham, Massachusetts), equipped with a 4-watt X-ray tube (Groover, 2016). The instrument measures concentrations of 27 elements; data for 18 of those elements, including chromium, were used in multivariate statistical analyses presented in this chapter. Samples of surficial alluvium were disaggregated where necessary, homogenized using the "rolling method" (U.S. Department of Agriculture, 1996; U.S. Environmental Protection Agency, 2007), and measured in sample cups designed for that purpose. Samples of rock and core material were measured on freshly exposed surfaces. Each measurement was done for 2 minutes across an oval area approximately 5 millimeters (mm) across its larger diameter according to methods described in U.S. Environmental Protection Agency (2007). Measurements were repeated at least three times for each sample, and the instrument was moved slightly between individual measurements to assess small-scale variations in sample composition. Measurements were optimized for high-chromium concentrations (greater than 200 mg/kg) by adjusting instrument settings according to manufacturer's specifications when high-chromium concentrations were encountered (Groover and Izbicki, 2019).

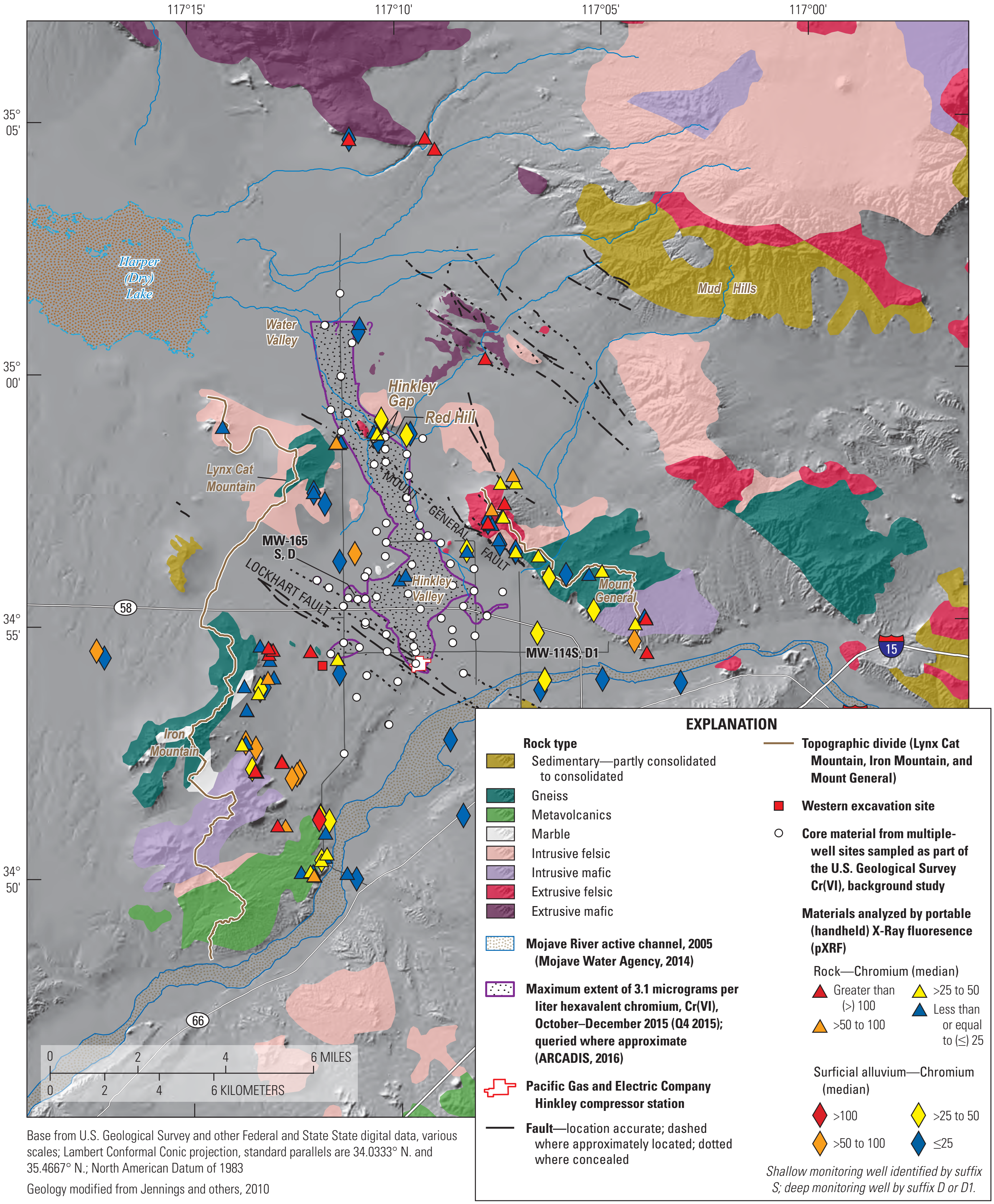

Base from U.S. Geological Survey and other Federal and State State digital data, various scales; Lambert Conformal Conic projection, standard parallels are 34.0333° N. and 35.4667° N.; North American Datum of 1983

Geology modified from Jennings and others, 2010

**Figure B.3.** Simplified bedrock geology and portable (handheld) X-ray fluorescence measurement sites for rock, alluvium, and core material from selected wells, Hinkley and Water Valleys, western Mojave Desert, California, 2015 through 2017. Site locations and data are available in Groover and Izbicki (2018).
]

Two National Institute of Standards and Technology (NIST) soil standards (2710a; National Institute of Standards and Technology, 2018; and 2711a, National Institute of Standards and Technology, 2022), a USGS rock standard (BHVO-2; U.S. Geological Survey, 2022), and a reagent-grade silica dioxide blank were measured daily prior to the beginning of data collection and routinely between selected samples using pXRF. Precision was calculated as the difference between the measured and standard concentrations divided by the standard concentration and expressed as a percent. The precision for chromium was 5.7 percent, and precision data for other trace elements are in table B.1. Elemental concentrations differed in each standard but approximated the range of environmental data. Silica blank data showed no evidence of contamination or sample carryover for chromium or most other trace elements measured; however, low concentrations of titanium and iron representing 0.7 and 0.05 percent of their respective concentrations in reagent-grade silica were present in some blank samples (Groover and Izbicki, 2018).

Portable (handheld) X-ray fluorescence data were compared with laboratory wavelength dispersive XRF (Phillips Magix Pro equipped with a 4,000-watt X-ray tube; WDXRF) data on splits from 33 samples collected from Hinkley and Water Valleys and other areas in the western Mojave Desert (Groover and Izbicki, 2019). Least-squared regression comparisons for pXRF and WDXRF chromium data showed good agreement, with an intercept not significantly different from 0 and a slope not significantly different from 1 (table B.2). Portable (handheld) X-ray fluorescence instrument values consistently overestimated vanadium concentrations in standards by 300 mg/kg; as a consequence, instrument vanadium concentrations were adjusted by subtracting 300 mg/kg to obtain the environmental concentration (Groover and Izbicki, 2019). The adjusted vanadium concentration was used in statistical analyses presented in this professional paper. Least-squares regression comparisons between pXRF and WDXRF data for other trace elements also are provided in table B.2.

Portable (handheld) X-ray fluorescence data also were compared with ICP-MS data from the USGS minerals laboratory in Denver, Colorado, on splits from 36 samples from Hinkley and Water Valleys and other areas in the western Mojave Desert (Morrison and others, 2018). Data collection and analytical methods for ICP-MS data are discussed in chapter C within this professional paper. In general, least-squares regression comparison showed good agreement for chromium analyzed by pXRF and ICP-MS, with a slope not significantly different from 1, an intercept not significantly different from zero, and a coefficient of determination ($R^2$) of 0.84 (table B.2). Least-squares regression comparisons between pXRF and ICP-MS data for other trace elements also are presented in table B.2.

The instrument reporting level for chromium on silica blanks was 2.4 mg/kg. Because of matrix interference with sample spectra, each measurement made using the pXRF effectively has a unique reporting level. A study reporting level (SRL) of 5 mg/kg, approximately twice the instrument reporting level, was used for data reporting and statistical purposes within this professional paper. The SRL is approximately equal to the mean square error (MSE) for the least-squares regression comparison of pXRF and WDXRF data, and approximately twice the MSE for the comparison of pXRF and ICP-MS data (table B.2). Data that were above the instrument reporting level but below the SRL were censored to values of less than 5 mg/kg for the purposes of this professional paper. Instrument and SRLs for other constituents measured by pXRF are provided in table B.1.

## B.3.2. Statistical Methods

Differences in elemental concentrations were evaluated on the basis of the median test (Neter and Wasserman, 1974); correlation coefficients were evaluated using Kendall's Tau β correlation coefficient (Kendall, 1938; Helsel and others, 2020). The statistical significance of differences and correlations were evaluated at a level of significance of 0.05 unless otherwise stated. Probability values (p-values) for individual tests are not provided. Median test results, correlation coefficients, and statistical distributions presented in this chapter were calculated using software from the SAS Institute (Cary, North Carolina). Regression analysis was done using the method of least-squares (Neter and Wasserman. 1974), regression statistics including slope, intercept, MSE, and $R^2$ were calculated using software from the SAS Institute. For quality assurance purposes, the significance of slope and intercept values, relative to expected values of 1 and 0 respectively, was evaluated on the basis of the t-test (Neter and Wasserman, 1974) at a level of significance of 0.05 unless otherwise stated. Intervals around regression lines were calculated according to methods described by Neter and Wasserman (1974) using Excel (Microsoft, Redmond, Washington).

Elemental concentration data from pXRF measurements were interpreted using principal component analysis (PCA) to evaluate elemental assemblages and co-occurrence in samples of surficial alluvium eroded from rock in different geologic source terrains with core material adjacent to the screened interval of sampled wells within Hinkley and Water Valleys. Principal component analysis results also were used to evaluate the effect of admixtures of local material eroded from local sources on the elemental composition of Mojave-type deposits within Hinkley and Water Valleys.

**Table B.1.** Quality-assurance data, mean, standard deviation, and eigenvectors used to calculate principal component scores for rock and core material, Hinkley and Water Valleys, California.

[Results from principal component analyses (PCA) of portable (handheld) X-ray fluorescence (pXRF) data on surficial alluvium (Groover and Izbicki, 2018). Numbers rounded for presentation. **Abbreviations**: mg/kg, milligram per kilogram; >, greater than; NIST, National Institute of Standards and Technology]

| Principal component | Calcium | Iron | Potassium | Titanium | Arsenic | Chromium | Copper | Lead | Manganese |
|---|---|---|---|---|---|---|---|---|---|
| | Major elements (mg/kg) | | | | Minor and trace elements (mg/kg) | | | | |
| Instrument reporting level | 4.5 | 5.7 | 99 | 32 | 0.9 | 2.4 | 2.3 | 1.4 | 3.2 |
| Study reporting level | 504 | 5.7 | 99 | 32 | 1.3 | 3.1 | 2.6 | 2.3 | 5.7 |
| Mean | 31,900 | 18,900 | 26,200 | 2,160 | 7.0 | 28 | 15 | 16 | 351 |
| Standard deviation | 25,500 | 15,600 | 11,500 | 1,380 | 7.2 | 34 | 15 | 14 | 234 |
| Precision, in percent[1] | 8.5 | 8.0 | 13 | 8.8 | 10 | 5.7 | 8.8 | 3.1 | 6.1 |
| Detection frequency, in percent | >99 | 100 | >99 | >99 | 89 | 94 | 96 | 93 | >99 |
| Eigenvectors (unitless) | | | | | | | | | |
| 1 | 0.33546 | 0.39743 | −0.07773 | 0.36199 | 0.22587 | 0.30335 | 0.32978 | −0.03230 | 0.38441 |
| 2 | −0.12106 | −0.05264 | 0.47629 | 0.01987 | 0.19234 | −0.07887 | 0.01050 | 0.37054 | 0.10181 |
| 3 | 0.02655 | 0.15275 | −0.03321 | −0.01356 | −0.36878 | 0.12861 | 0.12944 | 0.16666 | −0.06935 |
| 4 | −0.07510 | 0.03370 | −0.12365 | 0.22701 | −0.33599 | 0.06825 | −0.14071 | 0.00534 | −0.05475 |
| 5 | 0.06603 | −0.04597 | −0.02557 | −0.23371 | −0.02310 | −0.33160 | 0.08768 | 0.23115 | −0.13827 |
| 6 | −0.03624 | −0.18509 | 0.10041 | −0.07602 | 0.11782 | 0.32657 | −0.43047 | 0.02122 | 0.08628 |
| 7 | −0.11141 | 0.13334 | 0.05369 | 0.14699 | 0.16769 | −0.20202 | 0.23830 | −0.56987 | −0.10324 |
| 8 | −0.09597 | −0.08137 | 0.03169 | −0.13547 | 0.06969 | −0.11217 | 0.20590 | −0.25696 | −0.11292 |
| 9 | −0.42074 | −0.01387 | 0.11447 | 0.18668 | −0.02726 | 0.55709 | −0.16295 | −0.12181 | −0.01490 |
| 10 | 0.56291 | −0.06838 | −0.17155 | −0.21482 | −0.02553 | 0.08169 | −0.31190 | −0.02089 | 0.10952 |
| 11 | 0.44466 | −0.00016 | 0.28525 | −0.15602 | −0.06521 | 0.27308 | 0.19663 | −0.14622 | −0.30989 |
| 12 | −0.26080 | 0.14503 | −0.23801 | −0.12248 | −0.16522 | 0.15472 | 0.42096 | 0.40268 | −0.04653 |
| 13 | 0.06569 | −0.00214 | −0.06450 | −0.34121 | 0.23411 | 0.34916 | 0.22173 | 0.18076 | −0.11271 |
| 14 | 0.24479 | −0.20238 | −0.00214 | 0.66538 | 0.02071 | −0.05173 | −0.00999 | 0.28142 | −0.50424 |
| 15 | 0.05722 | 0.14979 | 0.14110 | 0.15352 | 0.07099 | −0.24997 | −0.07981 | 0.23337 | 0.48722 |
| 16 | 0.09608 | 0.06743 | 0.22623 | −0.00714 | −0.71930 | −0.02268 | 0.03444 | −0.13986 | 0.19069 |
| 17 | −0.03926 | 0.81222 | 0.09917 | −0.10797 | 0.06902 | −0.07711 | −0.38115 | 0.05828 | −0.36380 |
| 18 | 0.03549 | −0.02195 | 0.68590 | −0.04147 | −0.01815 | 0.03880 | 0.14357 | 0.03328 | −0.02493 |

**Table B.1.** Quality-assurance data, mean, standard deviation, and eigenvectors used to calculate principal component scores for rock and core material, Hinkley and Water Valleys, California.—Continued

[Results from principal component analyses (PCA) of portable (handheld) X-ray fluorescence (pXRF) data on surficial alluvium (Groover and Izbicki, 2018). Numbers rounded for presentation. **Abbreviations**: mg/kg, milligram per kilogram; >, greater than; NIST, National Institute of Standards and Technology]

| Principal component | Molybdenum[2] | Nickel | Rubidium | Strontium | Tin[2] | Uranium | Vanadium[3] | Zinc | Zirconium |
|---|---|---|---|---|---|---|---|---|---|
| Minor and trace elements (mg/kg) | | | | | | | | | |
| Instrument reporting level | 0.90 | 5.2 | 0.69 | 0.43 | 11.1 | 1.2 | 32 | 1.4 | 0.81 |
| Study reporting level | 1.2 | 6 | 1.2 | 1.3 | 11.1 | 2.0 | 30 | 1.7 | 1.7 |
| Mean | 1.3 | 29 | 111 | 458 | 12 | 1.8 | 113 | 38 | 176 |
| Standard deviation | 1.0 | 12 | 55 | 173 | 6.7 | 0.81 | 33 | 27 | 115 |
| Precision, in percent | 24 | 17 | 8.2 | 1.6 | 17 | 25 | 33 | 7.3 | 43 |
| Detection frequency, in percent[1] | 53 | 86 | 98 | >99 | 28 | 20 | >99 | 99 | 98 |
| Eigenvectors (unitless) | | | | | | | | | |
| 1 | 0.17699 | 0.16433 | −0.08111 | 0.19303 | 0.08810 | −0.05152 | 0.14674 | 0.23532 | 0.04840 |
| 2 | 0.09416 | −0.11539 | 0.47359 | −0.10374 | 0.01703 | 0.35439 | 0.17874 | 0.37026 | 0.11038 |
| 3 | −0.39803 | 0.34694 | −0.03950 | −0.39682 | 0.34334 | 0.20891 | 0.37443 | −0.05449 | −0.17404 |
| 4 | 0.32829 | 0.01405 | −0.09010 | −0.27213 | 0.01397 | 0.09005 | −0.00186 | −0.02455 | 0.76614 |
| 5 | 0.37949 | −0.03487 | −0.10296 | 0.36516 | 0.56607 | −0.14044 | 0.31435 | −0.12741 | 0.05613 |
| 6 | 0.12091 | 0.56588 | 0.09355 | 0.11502 | 0.36066 | 0.03444 | −0.38178 | 0.01381 | −0.02859 |
| 7 | −0.05393 | −0.15413 | 0.12885 | −0.09949 | 0.47866 | 0.33969 | −0.28057 | −0.08149 | 0.03402 |
| 8 | 0.07653 | 0.52015 | 0.03069 | 0.31181 | −0.39666 | 0.39724 | 0.27763 | −0.20065 | 0.13833 |
| 9 | 0.10964 | −0.33360 | −0.01480 | 0.20799 | 0.06901 | 0.09070 | 0.35492 | −0.30202 | −0.15866 |
| 10 | 0.07803 | −0.28498 | −0.15708 | 0.01846 | −0.01370 | 0.60339 | 0.03074 | −0.03202 | −0.08538 |
| 11 | 0.32265 | 0.00264 | 0.37511 | −0.26931 | −0.07795 | −0.23711 | −0.00527 | −0.27728 | −0.07153 |
| 12 | 0.32162 | −0.02792 | −0.02294 | 0.00567 | −0.08013 | 0.28455 | −0.44495 | −0.08227 | −0.22281 |
| 13 | −0.49587 | −0.15118 | 0.07323 | 0.21841 | 0.09585 | −0.02088 | −0.09909 | −0.11960 | 0.49828 |
| 14 | −0.15328 | 0.02762 | 0.02012 | 0.24103 | −0.00971 | 0.11253 | −0.11155 | −0.09413 | −0.05393 |
| 15 | −0.08895 | 0.02198 | 0.12426 | −0.05572 | −0.03020 | 0.00315 | −0.09107 | −0.72499 | 0.05749 |
| 16 | −0.15181 | −0.06934 | 0.24782 | 0.47659 | 0.00636 | −0.01405 | −0.16473 | 0.12528 | 0.02247 |
| 17 | −0.01331 | 0.03402 | 0.01277 | 0.11346 | −0.09451 | 0.02054 | −0.03937 | 0.01550 | −0.00425 |
| 18 | −0.00646 | −0.00511 | −0.68822 | −0.04117 | −0.01711 | 0.05173 | −0.14760 | −0.00543 | 0.04137 |

[1] Precision calculated as the average precision of measurements for the NIST soil standards 2710a and 2711a and the U.S. Geological Survey rock standard BHVO-2 expressed as a percent of the standard's nominal value. Elemental concentrations differ in each standard but approximate the range of environmental data.

[2] Molybdemun and tin were not quantified in NIST soil standards or U.S. Geological Survey rock standards. Precision was calculated as the average concentration divided by the standard deviation, expressed as a percent.

[3] Measured vanadium concentrations adjusted on the basis of standard data by subtracting 300 mg/kg (Groover and Izbicki, 2019). A study reporting level of 30 mg/kg was used for adjusted vanadium concentrations.

**Table B.2.** Comparison between selected elemental concentrations in surficial alluvium and core material measured using portable (handheld) energy dispersive X-ray fluorescence (pXRF), laboratory wavelength dispersive X-ray fluorescence (WDXRF), and inductively coupled plasma-mass spectrometry (ICP-MS) data, Hinkley and Water Valleys, California, 2015 to 2018.

[Regression statistics calculated from data in Groover and Izbicki (2018) and Morrison and others (2018). Numbers rounded for presentation. **Abbreviations**: mg/kg, milligram per kilogram; $R^2$, coefficient of determination ranges from 0 for no relation to 1 for a perfect correlation; —, no data]

| Element | Least-squares regression statistics with pXRF as the dependent variable and indicated independent variable | | | | | | | |
|---|---|---|---|---|---|---|---|---|
| | Laboratory wavelength dispersive X-ray fluorescence (WDXRF) | | | | Inductively coupled plasma-mass spectrometry (ICP-MS) | | | |
| | Slope (mg/kg pXRF/ mg/kg WDXRF) | $R^2$ (unitless) | Mean squared error (mg/kg) | Intercept (mg/kg) | Slope (mg/kg pXRF/ mg/kg ICP-MS) | $R^2$ (unitless) | Mean squared error (mg/kg) | Intercept (mg/kg) |
| Arsenic (As) | — | — | — | — | 0.84 | 0.80 | 0.59 | 1.0 |
| Calcium (Ca) | 1.4 | 0.90 | 1.1 | −7,950 | 1.2 | 0.78 | 3,980 | −2,510 |
| Chromium (Cr) | 1.04 | 0.84 | 5.1 | 1.4 | 1.00 | 0.97 | 2.3 | 8.9 |
| Copper (Cu) | 0.79 | 0.94 | 0.85 | 2.4 | 0.92 | 0.40 | 4.5 | 1.7 |
| Iron (Fe) | 1.7 | 0.90 | 1.4 | 380 | 0.81 | 0.68 | 2,940 | 2,900 |
| Lead (Pb) | 0.66 | 0.31 | 3.5 | 2.8 | 0.51 | 0.66 | 2.3 | 2.8 |
| Manganese (Mn) | 0.91 | 0.91 | 0.01 | 1.9 | 0.90 | 0.69 | 64 | −14 |
| Molybdenum (Mo) | 0.73 | 0.88 | 0.83 | 1.7 | 0.22 | 0.13 | 0.18 | 2.1 |
| Nickel (Ni) | 0.78 | 0.89 | 1.8 | 20 | 1.1 | 0.77 | 3.4 | 11 |
| Potassium (K) | 0.94 | 0.52 | 0.56 | 11,600 | 0.82 | 0.90 | 1,560 | 1,830 |
| Rubidium (Rb) | 0.94 | 0.92 | 4.3 | 10 | 1.1 | 0.93 | 6.5 | −11 |
| Strontium (Sr) | 0.98 | 0.95 | 18 | 51 | 1.3 | 0.70 | 67 | −76 |
| Tin (Sn) | — | — | — | — | 1.3 | 0.06 | 1.97 | 15 |
| Titanium (Ti) | 0.95 | 0.73 | 0.14 | −23 | 0.67 | 0.63 | 294 | 710 |
| Uranium (U) | 1.00 | 0.95 | 0.52 | 2.1 | 0.84 | 0.82 | 0.393 | 2.2 |
| Vanadium (V) | 1.05 | 0.66 | 13 | 300 | 0.69 | 0.09 | 40.5 | 340 |
| Zinc (Zn) | 0.79 | 0.98 | 2.0 | 0.85 | 0.75 | 0.75 | 5.2 | 3.8 |
| Zirconium (Zr) | 1.3 | 0.91 | 13 | 11 | 1.6 | 0.88 | 19.6 | −60 |

Principal component analysis is a multivariate technique that uses matrix algebra to transform potentially correlated and potentially non-linear data (in this case, elemental concentrations of alluvium measured using pXRF) into new variables, which are uncorrelated linear combinations of the original data (Hotelling, 1933; Wold and others, 1987). The new variables are called principal components, and there is one principal component for each variable in the original dataset. The magnitude of the principal components for each measurement within the dataset is called a score. Principal component scores are calculated from eigenvectors estimated by PCA. Eigenvectors for each principal component range from −1 to 1 and describe the direction (positive or negative) and magnitude of the contribution of the original data (in this case, pXRF elemental concentration data) to the principal component scores. Calculations within PCA are solely algebraic without any underlying statistical assumptions, and principal components preserve exactly the variability within the original data. Multivariate statistics, such as PCA, are commonly used to interpret elemental concentration data from geologic materials (Grunsky and de Caritat, 2019).

Principal component scores for surficial alluvium were calculated using software from the SAS Institute (Cary, North Carolina). Principal component scores for rocks ($S_{rn}$) were calculated from mean, standard deviation, and eigenvector data for surficial alluvium (table B.1) according to the following equation:

$$S_{rn} = \sum \left\{ \left( \frac{X_{r_\gamma} - \overline{X}_{a_\gamma}}{\sigma_{a_\gamma}} \right) * \vec{E}_{\gamma n} \right\} \qquad \text{(B.1)}$$

where

$a$ = alluvium, $r$ = rock; $\gamma$ = is the individual element (table B.2),

$X_{r_\gamma}$ = concentration of element $\gamma$ for a given rock measurement,

$\overline{X}_{a_\gamma}$ = mean concentration of element $\gamma$ in alluvium measurements,

$\sigma$ = standard deviation from the mean for element $\gamma$ in alluvium; and

$\vec{E}$ = $n$th eigenvector for element $\gamma$ where $n$ = 1, 2, 3, ....

Scores calculated for pXRF data from surficial alluvium were compared with scores calculated for rock data to verify PCA results with respect to identification of different geologic source terrains. After assessing the suitability of the comparison, scores were calculated for pXRF data from core material adjacent to the screened interval of wells, in a manner similar to scores for rocks (eq. B.1), to identify the geologic source of materials penetrated by wells that are often difficult to evaluate directly.

By design, data for PCA within this professional paper were not normalized prior to analyses. Normalization of data (adjusting values of variables in a dataset so they have the same standard deviation) is commonly done to ensure that PCA results using different types of data, expressed in different units, are not dominated by scale differences between the variables. In this professional paper, pXRF data for surficial alluvium are a similar type (elemental concentrations) and are measured in the same units (mg/kg), so scale differences between variables are not a concern. Additionally, normalization artificially reduces variability within data prior to analysis and may obscure variations associated with measured concentrations. Statistical moments (mean and standard deviation) and PCA eigenvectors from surficial alluvium can be used to characterize additional data collected in the future, providing a tool to allow interpretation of additional data as they are collected without redoing the PCA.

# B.4. Chromium Concentrations in Rock, Surficial Alluvium, and Core Material

Chromium concentrations in rock, surficial alluvium, and core material were evaluated on the basis of more than 1,500 pXRF measurements on more than 250 samples of rock, surficial alluvium, and core material from selected wells (Groover and Izbicki, 2018). Manganese concentrations in core material and the correlation between chromium and manganese, which can oxidize trivalent chromium, Cr(III), to Cr(VI) (Schroeder and Lee, 1975) also were examined. Geochemical exploration techniques were adapted to evaluate high concentrations of chromium and manganese in core material adjacent to the screened interval of sampled wells (fig. B.2; chapters E and F) and to identify threshold concentrations for use within a summative-scale analysis (SSA) later in this professional paper (chapter G) that may be associated with high natural concentrations of Cr(VI) in water from those wells.

## B.4.1. Chromium Concentrations in Rock

Chromium concentrations from almost 200 pXRF measurements on more than 60 samples of rock in Hinkley and Water Valleys (fig. B.3) ranged from less than the SRL of 5 to 900 mg/kg (table B.3), with a median concentration of 26 mg/kg. Although some rocks in Hinkley and Water Valleys have chromium concentrations greater than the average bulk continental abundance for chromium of 185 mg/kg (Reimann and de Caritat, 1998), chromium concentrations of rocks in Hinkley and Water Valleys are low compared to chromium concentrations as high as 8,600 mg/kg in mafic Pelona Schist that crops out in the San Gabriel Mountains west of the study area (table B.3). High chromium concentrations in mafic rock in the San Gabriel Mountains were identified previously by Izbicki and others (2008). Erosion of mafic rock from the San Gabriel Mountains, such as the Pelona Schist, contributed alluvium to the Mojave River from 1 to 3 million years ago (prior to geologic movement of the San Gabriel Mountains along the San Andreas Fault and the geologic development of Cajon Pass).This alluvium was subsequently transported to and deposited in Hinkley and Water Valleys (Groover and Izbicki, 2019).

**Table B.3.** Chromium concentrations in selected rocks, Hinkley and Water Valleys, western Mojave Desert, California.

[Data are from handheld X-ray fluorescence data in Groover and Izbicki (2018); values rounded from instrument readings. **Abbreviations**: mg/kg, milligram per kilogram; —, not a mappable unit; <, less than]

| Generalized area, simplified geologic unit, and rock type[1] | Surface exposure in Hinkley and Water Valleys (acres) | Number of measurements | Minimum | Median | Maximum |
|---|---|---|---|---|---|
| | | | | (mg/kg) | |
| **Iron Mountain (total 9,000 acres)** | 3,700 | — | — | — | — |
| Igneous rock | | | | | |
| Intrusive mafic (hornblende diorite, diorite) | 1,260 | 22 | 11 | 84 | 530 |
| Intrusive mafic (basalt, diabase dikes) | — | 16 | 20 | 410 | 900 |
| Intrusive felsic (quartz diorite, granite) | 111 | 12 | <5 | <5 | 15 |
| Metamorphic rock | | | | | |
| Gneiss | 888 | 14 | 22 | 37 | 170 |
| Marble | 259 | 9 | <5 | <5 | <5 |
| Miscellaneous (metavolcanics, mica schist) | 1,180 | 30 | <5 | 26 | 72 |
| **Mount General (total 6,000 acres)** | 2,180 | — | — | — | — |
| Igneous rock | | | | | |
| Intrusive mafic (hornblende diorite, diorite) | 240 | 9 | <5 | 29 | 320 |
| Intrusive felsic (quartz diorite, granite) | 327 | 9 | <5 | <5 | 20 |
| Extrusive felsic (rhyolite, dacite) | 654 | 23 | 10 | 28 | 64 |
| Metamorphic rock | | | | | |
| Gneiss | 937 | 18 | <5 | 24 | 180 |
| Marble | <20 | 3 | <5 | <5 | <5 |
| Miscellaneous (metavolcanics) | <20 | 7 | <5 | 38 | 84 |
| Hydrothermally altered | <20 | 18 | 20 | 48 | 350 |
| **Other areas** | | | | | |
| Lynx Cat Mountain (total 2,960 acres) | 2,050 | — | — | — | — |
| Igneous (intrusive felsic) | 1,370 | 11 | <5 | 12 | 51 |
| Metamorphic (undifferentiated) | 656 | 15 | <5 | 11 | 61 |
| Red Hill (extrusive felsic, intrusive felsic) | 64 | 6 | 14 | 21 | 47 |
| Basalts (Water Valley) | Areally extensive | 15 | 110 | 180 | 310 |
| Other (Including bedrock knobs, Hinkley Valley) | 50 | 30 | <5 | 18 | 310 |
| **Geologic materials outside Hinkley and Water Valleys** | | | | | |
| Mafic rock (Pelona Schist, San Gabriel Mountains) | — | 11 | 160 | 4,600 | 8,600 |
| | | | | **Typical value (mg/kg)** | |
| Bulk continental abundance (Reimann and de Caritat, 1998) | | | | 185 | |
| Ultramafic rock (Reimann and de Caritat, 1998) | | | | 2,300 | |
| Basalt (Reimann and de Caritat, 1998) | | | | 250 | |

[1] Geologic units and areal extent of units simplified from Jennings and others (2010). Rock type from field descriptions (Groover and Izbicki, 2018).

Chromium concentrations in rocks within Hinkley and Water Valleys are highest in basalt, intruded within marble in the northern part of Iron Mountain (table B.3). This intrusive basalt (fig. B.4) is present only as thin dikes within the marble, has limited areal extent, and is not mapped as a discrete unit (fig. B.3). Chromium concentrations are as high as 530 mg/kg, with a median concentration of 84 mg/kg (table B.3), in intrusive mafic rock (hornblende diorite and diorite; fig. B.4), which crops out over 34 percent of the east slope of Iron Mountain that drains toward Hinkley Valley (fig. B.3). Chromium concentrations are as high as 170 mg/kg (table B.3) in gneiss, which crops out over 24 percent of the east slope of Iron Mountain. However, this gneiss is not consistently high in chromium and has a median concentration of 37 mg/kg (table B.3). Intrusive felsic rock (such as quartz diorite and granite), marble, and other miscellaneous metamorphic rock (such as metavolcanics and mica schist), which collectively crop out over 42 percent of the east slope of Iron Mountain, have lower chromium concentrations, commonly less than 5 mg/kg (table B.3). Mafic and gneissic bedrock similar to rocks that crop out on Iron Mountain underlie much of the western and northern parts of Hinkley Valley south of the Mount General fault and are present in core material from wells that penetrate bedrock in those areas (Miller and others, 2020).

Intrusive mafic rocks also crop out on the southern part of Mount General. Chromium concentrations in these rocks are slightly lower than similar rocks from Iron Mountain, with a maximum concentration of 320 mg/kg and a median concentration of 29 mg/kg (table B.3). Intrusive mafic rocks crop out over 11 percent of the western slope of the southern part of Mount General that drains toward Hinkley Valley (fig. B.3). In recent geologic time, since the Mojave River flowed past Barstow to create and maintain Lake Manix (not shown on fig. B.2) about 500,000 years ago (Reheis and others, 2012), material eroded from the southern part of Mount General would largely have been transported out of Hinkley Valley by the Mojave River. Chromium concentrations are as high as 180 mg/kg in gneiss that crops out over 43 percent of the west slope of Mount General (table B.3). However, similar to gneiss that crops out on Iron Mountain, these rocks are not consistently high in chromium, with median chromium concentrations of 24 mg/kg. Volcanic rock (dacite and rhyolite) that crop out over 30 percent of the west slope of Mount General, thought to be a potential source of chromium, have concentrations as high as 64 mg/kg, with a median chromium concentration of 28 mg/kg (table B.3).

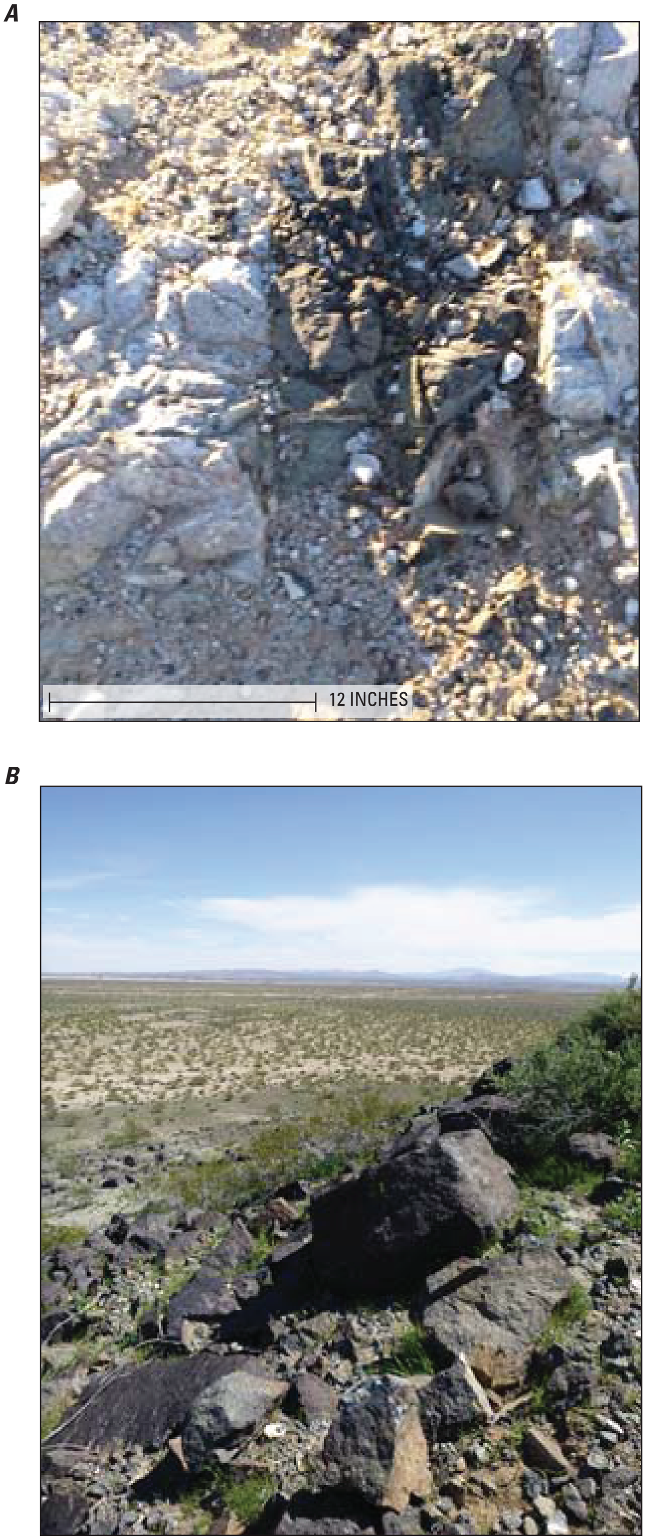

**Figure B.4.** Chromium-containing rock *A,* basalt dike in marble and *B,* hornblende diorite, Iron Mountain, Hinkley Valley, western Mojave Desert, California. (Photographs by Krishangi Groover, U.S, Geological Survey, July 2017.)

Although chromium concentrations in Mount General are not as high as concentrations on Iron Mountain, Mount General is extensively mineralized with high concentrations of other elements, including arsenic, copper, lead, silver, uranium, vanadium, and zinc (Housley and Reynolds, 2002). Some mineralized hydrothermal rocks from Mount General have chromium concentrations as high as 350 mg/kg, arsenic concentrations as high as 1,400 mg/kg, and uranium concentrations as high as 180 mg/kg. For comparison, the average bulk continental abundance of arsenic and uranium are 1 and 0.9 mg/kg, respectively (Taylor and McLennan, 1995). Similar to intrusive basalt within marble outcrops on Iron Mountain, hydrothermal rock on Mount General is not areally extensive, and is not mapped as a discrete unit (fig. B.3).

Chromium concentrations in felsic and metamorphic (including gneiss) rock that crop out on Lynx Cat Mountain and Red Hill, in the northern part of Hinkley Valley and the southern part of Water Valley (fig. B.3), are low with median concentrations of 12 and 11 mg/kg, respectively (table B.3). Basalts that crop out extensively within Water Valley are consistently near or higher than the average bulk continental abundance for chromium, with chromium concentrations ranging from 108 to 310 mg/kg and a median concentration of 180 mg/kg (table B.3). In some areas, basalt flows are interbedded with alluvial deposits (Ninyo and Moore, 2009; Stantec, 2013), and basalt fragments were commonly present in core material from wells in Water Valley (Groover and Izbicki, 2018; Miller and others, 2020). Basalts are not present in Hinkley Valley near the Hinkley compressor station (fig. B.3).

Bedrock knobs within Hinkley Valley, composed of metamorphic rock (including gneiss, marble, and other miscellaneous metamorphic rock), or extrusive volcanic rock near Mount General, have generally low chromium concentrations, with a median concentration of 18 mg/kg. Chromium concentrations as high as 310 mg/kg (table B.3) were measured in intrusive mafic rock (hornblende diorite) in a knob near Iron Mountain (fig. B.3). However, the bedrock knob closest to the “western excavation site,” an area associated with chromium-containing groundwater above the 3.1 µg/L interim regulatory background (Lahontan Regional Water Quality Control Board, 2014), had a median chromium concentration of 26 mg/kg (table B.3), with a maximum concentration of 45 mg/kg in a small inclusion within the host gneiss (Groover and Izbicki, 2018).

## B.4.2. Chromium Concentrations in Surficial Alluvium

Elemental concentrations in rock in complex geologic settings often differ across short distances. As a consequence, it can be difficult to sample rocks to obtain data representative the larger geologic source terrain. In contrast, samples from alluviated stream channels and alluvial fans integrate (by physical mixing within the stream channel) material eroded from rocks in upstream source terrains. Elemental concentrations from alluvial deposits often provide a more representative average approximation of elemental concentrations and co-occurrence within the larger area upstream of the sample location than data from rock or soil (Chaffee, 1975; Painter and others, 1994). This is especially true for alluviated stream channels in desert areas where erosion, dominated by mechanical processes, predominates, and chemical changes associated with mineral weathering, leaching, and soil development in surficial alluvium within active stream channels are less important.

Chromium concentrations in 179 measurements on more than 55 samples of surficial alluvium from alluviated stream channels draining Iron Mountain, Mount General, Lynx Cat Mountain, and other areas within Hinkley and Water Valleys (fig. B.3) ranged from less than the SRL of 5 to 295 mg/kg, with a median concentration of 22 mg/kg (fig. B.5). Concentrations are generally lower in material within alluviated stream channels than in rock because of physical mixing and averaging of material from different sources (Chaffee, 1975; Painter and others, 1994; Groover and Izbicki, 2019).

Surficial alluvium eroded from rocks that crop out on Iron Mountain has a median concentration of 48 mg/kg and a maximum concentration of 295 mg/kg in alluvium eroded from hornblende diorite (fig. B.5). Four samples of alluvium eroded from Iron Mountain have chromium concentrations greater than 100 mg/kg. However, not all alluvium eroded from Iron Mountain is high in chromium, and chromium concentrations less than 5 mg/kg were measured in alluvium eroded from intrusive felsic and miscellaneous metamorphic rock that compose the southern part of Iron Mountain near the channel of the Mojave River (fig. B.3).

Median chromium concentrations in surficial alluvium eroded from Mount General and Lynx Cat Mountain in Hinkley and Water Valleys of 20 and 22 mg/kg, respectively (fig. B.5), were significantly different from median chromium concentrations in alluvium eroded from Iron Mountain. Alluvium eroded from basaltic terrain in the Water Valley area is not well represented in pXRF data. Most stream channels draining basaltic terrain are not alluviated; where unconsolidated material is present within these channels, it is largely aeolian material from Harper (dry) Lake and has low chromium concentrations. Some alluvium in Water Valley was eroded from Miocene continental deposits within the Mud Hills (fig. B.3) east of the study area; these continental deposits have low chromium concentrations less than 8 mg/kg (Groover and Izbicki, 2018).

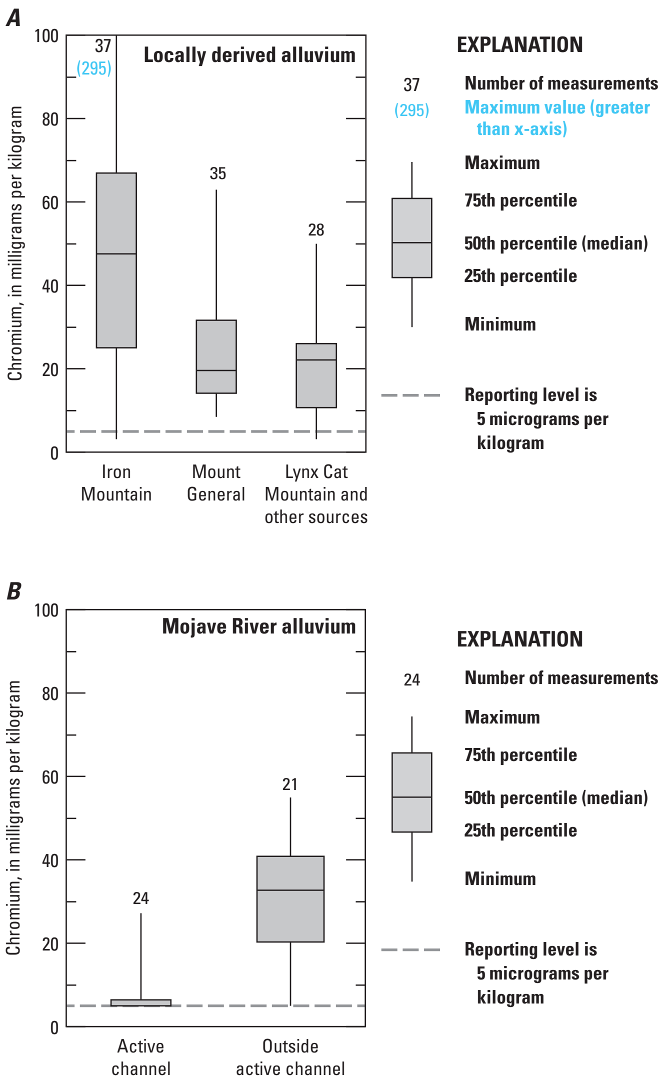

**Figure B.5.** Chromium concentrations in surficial alluvium eroded from *A,* Iron Mountain, Mount General, and other areas; and *B,* recent (active channel) and older Mojave River alluvium, Hinkley and Water Valleys, western Mojave Desert, California. Data are available in Groover and Izbicki (2018).

Most of the unconsolidated deposits in Hinkley and Water Valleys were sourced from the Mojave River (Miller and others, 2018, 2020), rather than from local sources such as Iron Mountain or Mount General. In the geologic past, erosion of high-chromium, mafic rock in the San Gabriel Mountains, such as the Pelona Schist (table B.3), contributed alluvium to the Mojave River (Groover and Izbicki, 2019). As a result of changes in the alluvial source area through recent geologic time, Mojave River alluvium in the western subarea has a median chromium concentration of 33 mg/kg. This value was significantly lower than median chromium concentrations in alluvium eroded from Iron Mountain (38 mg/kg) and significantly higher than median chromium concentrations in alluvium eroded from Mount General and Lynx Cat Mountain (20 and 22 mg/kg, respectively; fig. B.5). In contrast, recent alluvium from the active channel of the Mojave River, eroded from low-chromium intrusive felsic rock (primarily quartz monzonite) in the San Bernardino Mountains, had a median chromium concentration less than 5 mg/kg (fig. B.5).

## B.4.3. Chromium Concentrations in Core Material

More than 1,080 pXRF measurements were done on core material from 100 wells at selected sites (fig. B.3; Groover and Izbicki, 2018). Of those, more than 490 pXRF measurements were done on core material adjacent to the screened intervals of 79 wells sampled and analyzed for water chemistry (chapter E) and isotope composition (chapter F) in Hinkley and Water Valleys as part of this study (fig. B.2). Water from more than 100 wells was sampled and analyzed as part of this study, but core material was not available for pXRF analyses for domestic wells or for most monitoring wells drilled before 2011.

Lithology of aquifer material adjacent to the screened interval of sampled wells included coarse-gravel, sand, silt, and clay. Depositional provenances (Miller and others, 2018, 2020) included Mojave River stream, lake-margin, local alluvial fan deposits, lake (lacustrine), mudflat/playa, and groundwater discharge deposits (chapter A, table A.1). Weathered bedrock also was present adjacent to the screened interval of some sampled wells. Mojave River stream and lake-margin provenances represent Mojave-type deposits eroded from the San Bernardino Mountains (and in part from the San Gabriel Mountains for geologically older deposits), transported to and deposited within Hinkley and Water Valleys by the Mojave River. The areal and vertical distribution of depositional provinces interpreted from core material in PG&E monitoring wells as part of this study is discussed by Miller and others (2020). Most wells were screened across more than one lithology, and in many cases across more than one depositional provenance (Groover and Izbicki, 2018). Some wells were screened in intervals where aquifer material had been altered by weathering or by the formation of secondary minerals, including (1) calcite deposited within former groundwater-discharge areas near the toe of buried alluvial fan deposits (groundwater-discharge deposits) or (2) visually abundant iron or manganese oxides formed on the surfaces of mineral grains near redox boundaries associated with geologic contacts, lithologic contacts, or the water table.

Chromium concentrations in core material adjacent to the screened intervals of sampled wells ranged from less than the SRL of 5 to 410 mg/kg (fig. B.6), with a median concentration of 23 mg/kg. Median concentrations in core material were lower in the eastern subarea (20 mg/kg) and Water Valley (23 mg/kg), and median concentrations were higher in the northern (27 mg/kg) and western subareas (33 mg/kg; fig. B.7). Median chromium concentrations in the eastern subarea were significantly different from median concentrations in the western and northern subareas. Chromium concentrations were lowest in core material from wells completed in coarser-textured Mojave River stream deposits, with median concentrations ranging from 14 to 16 mg/kg (fig. B.7). Median chromium concentrations in all three subareas and in Water Valley increased as depositional provenance changed from generally coarse-textured Mojave River stream to lake margin to mudflat/playa deposits as the materials became finer-textured. In addition to changes in chromium concentrations with depositional provenance, chromium concentrations within Mojave River stream (fig. B.8*A*) and lake-margin provenances (fig. B.8*B*) also increased in finer-textured material.

Median chromium concentrations in fine-textured mudflat/playa deposits in the eastern subarea were 38 mg/kg (fig. B.7), with concentrations as high as 76 mg/kg in mudflat/playa deposits penetrated by well MW-199S1 near Mount General (fig. B.6). Median chromium concentrations in mudflat/playa deposits in the northern subarea were 45 mg/kg (fig. B.7), with concentrations as high as 85 and 75 mg/kg in core material adjacent to the screened interval of wells MW-133S1 and MW-154S1, respectively (fig. B.6). Although chromium concentrations in mudflat/playa deposits in the western subarea and Water Valley were similar to concentrations in the northern subarea, mudflat/playa deposits were encountered less frequently by sampled wells in the western subarea and Water Valley than elsewhere in the study area. Mineralogy of mudflat/playa deposits in the eastern and northern subareas were examined as a potential source of Cr(VI) in water from wells in greater detail in chapter C within this professional paper.

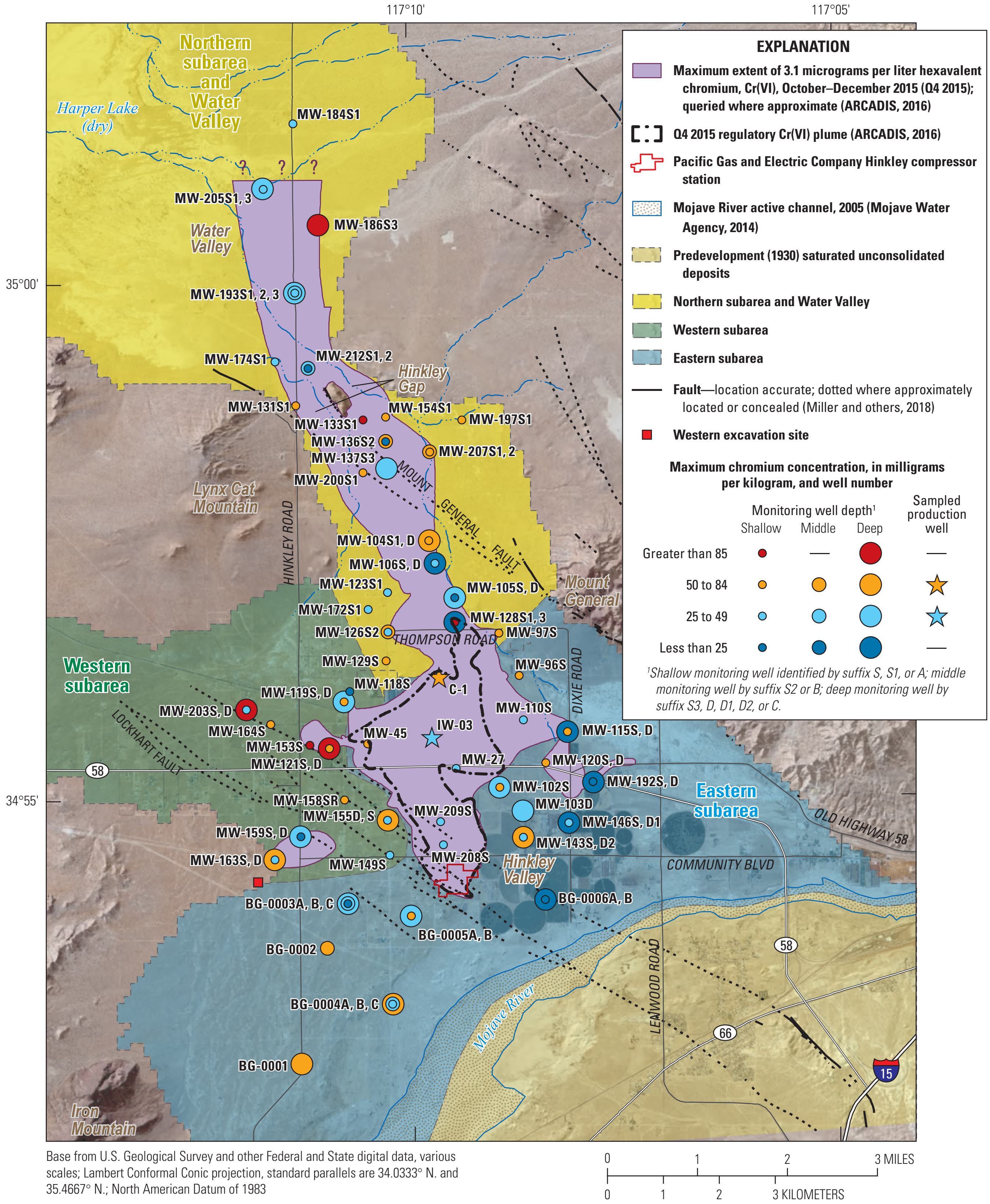

Base from U.S. Geological Survey and other Federal and State digital data, various scales; Lambert Conformal Conic projection, standard parallels are 34.0333° N. and 35.4667° N.; North American Datum of 1983

**Figure B.6.** Chromium concentrations in aquifer material adjacent to the screened interval of sampled wells, Hinkley and Water Valleys, western Mojave Desert, California, 2015 through 2018. Statistics were calculated from data available in Groover and Izbicki (2018).

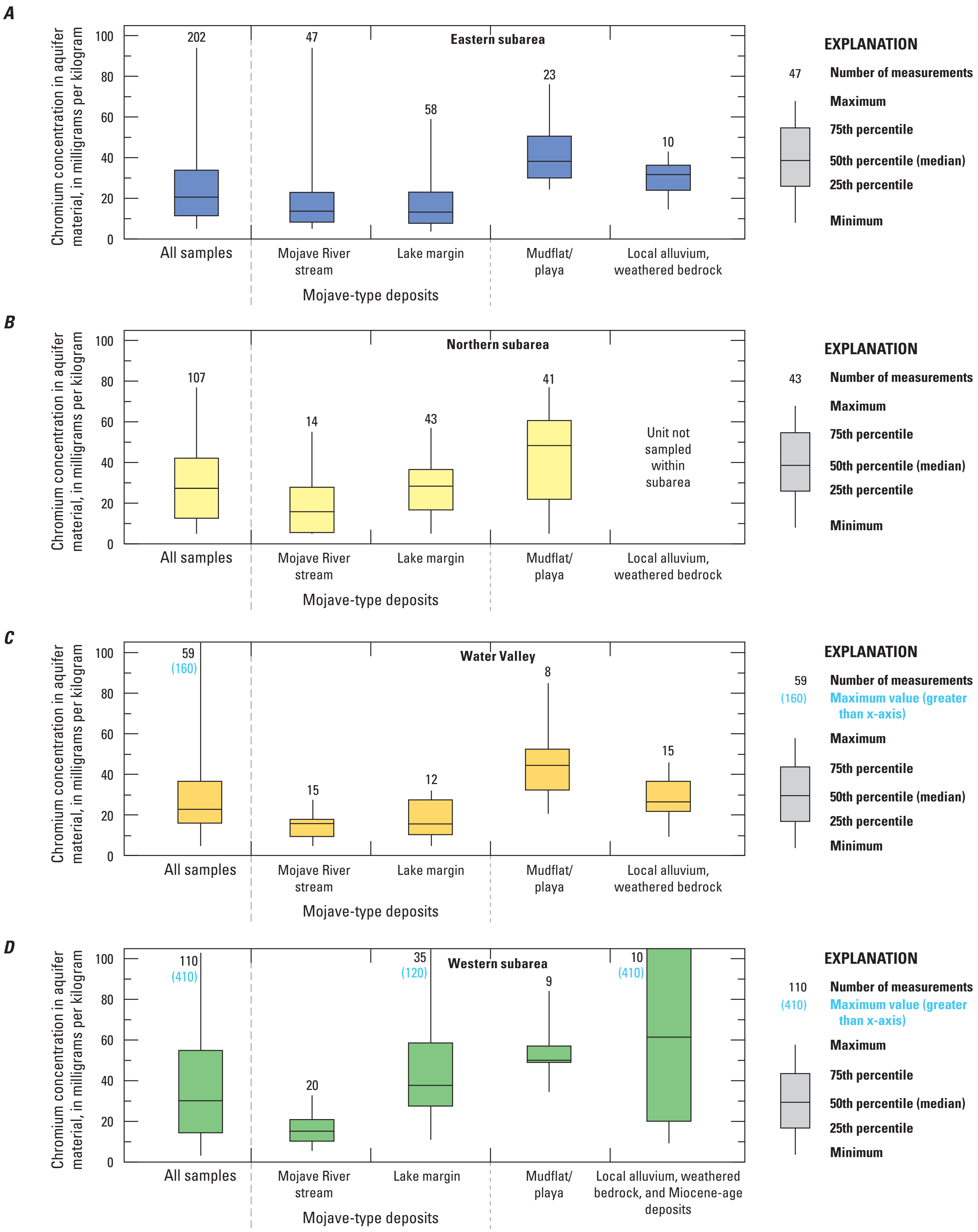

**Figure B.7.** Chromium concentrations in aquifer material, by depositional provenance adjacent to the screened interval of wells sampled in the *A,* eastern subarea, *B,* northern subarea, *C,* Water Valley, and *D,* western subarea, Hinkley and Water Valleys, western Mojave Desert, California, 2015 through 2018. Data are available in Groover and Izbicki (2018).

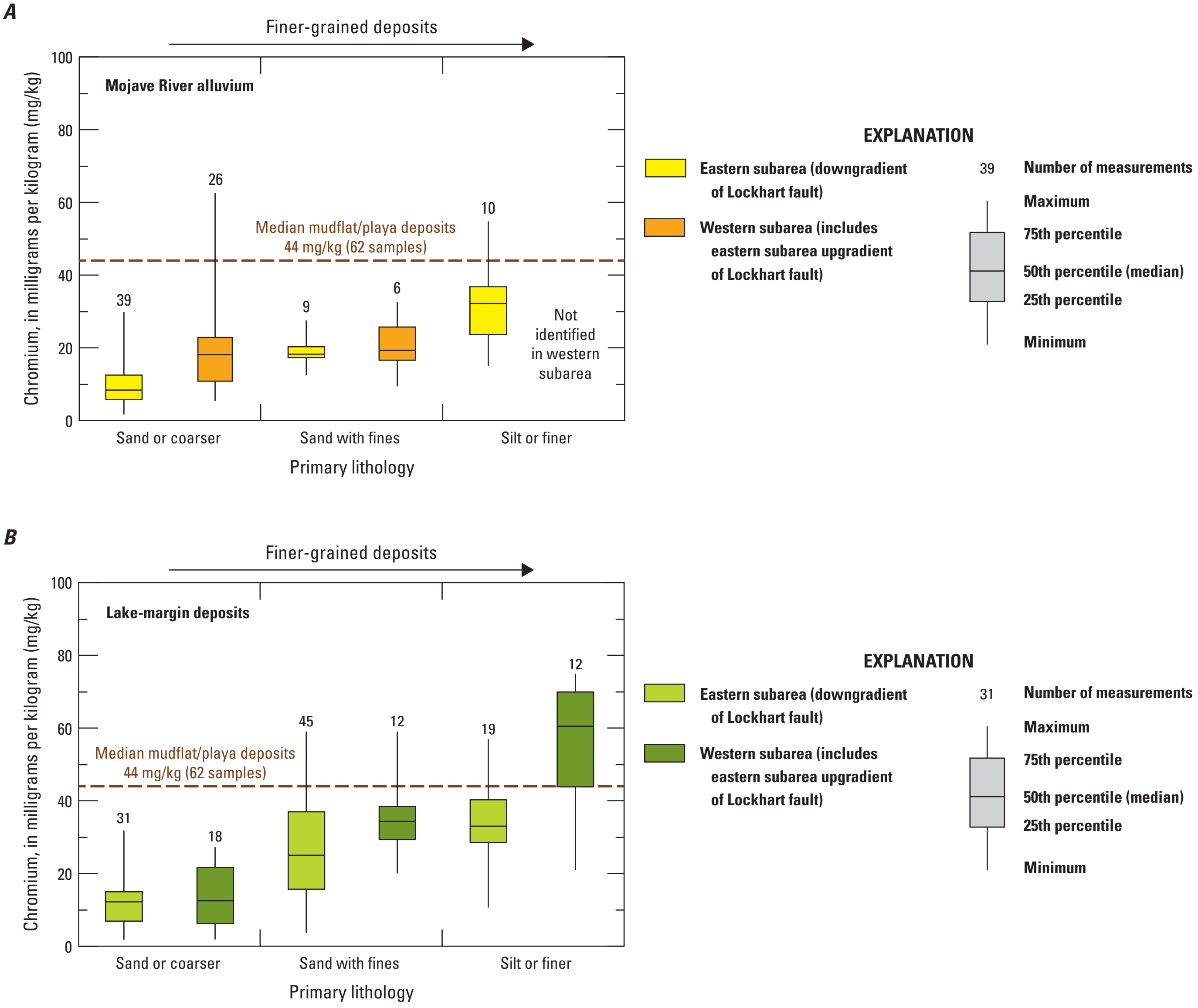

**Figure B.8.** Chromium concentrations by texture in Mojave-type deposits, including *A,* Mojave River alluvium and *B,* lake-margin deposits, adjacent to the screened interval of wells sampled in Hinkley and Water Valleys, western Mojave Desert, California, 2015 through 2018. Data are available in Groover and Izbicki (2018).

Median chromium concentrations in locally derived alluvium and weathered bedrock were commonly lower than concentrations in mudflat/playa deposits but higher than concentrations in Mojave-type deposits, except in the western subarea where chromium concentrations in locally derived alluvium and weathered bedrock ranged widely (fig. B.7). Chromium concentrations adjacent to the screened intervals of wells MW-153S and MW-203D completed in weathered mafic hornblende diorite bedrock (fig. B.9) and Miocene deposits underlying unconsolidated deposits in the western `subarea were as high as 405 and 347 mg/kg, respectively (fig. B.6). Chromium concentrations were as high as 120 mg/kg in fine-textured lake-margin deposits having visually abundant iron- and manganese-oxide coatings on the surfaces of mineral grains adjacent to the screened interval of well MW-121D in the western subarea (fig. B.10). Well MW-121D overlies mafic weathered bedrock, similar to material penetrated by MW-153S. Visually abundant iron- and manganese-oxide coatings on the surfaces of mineral grains in well MW-121D (fig. B.10) may have developed in response to differences in redox conditions near the geologic contact with chromium-containing hornblende diorite.

**Figure B.9.** Weathered hornblende diorite adjacent to the screened interval of well MW-153S, western subarea, Hinkley Valley, western Mojave Desert, California. (Photograph by Krishangi Groover, U.S. Geological Survey, March 2015.)

**Figure B.10.** Visually abundant secondary iron- and manganese-oxide coatings on core material adjacent to the screened interval of well MW-121D, western subarea, Hinkley Valley, California. (Photograph by Krishangi Groover, U.S. Geological Survey, July 2015.)

Median chromium concentrations in lake deposits were 35 mg/kg (not shown on fig. B.7; Groover and Izbicki, 2018). These materials compose the blue clay (chapter A, fig. A.6) and were generally deposited prior to the arrival of the Mojave River in Hinkley Valley (chapter A, fig. A.5). The blue clay is reduced, and pore fluids associated with these deposits are not associated with high concentrations of Cr(VI). Chromium concentrations ranging from 145 to 155 mg/kg associated with lake deposits containing basaltic fragments were present in core material adjacent to the screened interval of MW-186S3 in Water Valley. Median chromium concentrations in buried groundwater-discharge deposits were 16 mg/kg (not shown on fig. B.7; Groover and Izbicki, 2018). These calcite-rich, fine-textured materials were formed as a result of groundwater discharge near the toe of alluvial fans (chapter A, fig. A.5). Although generally low in chromium, concentrations were as high as 45 mg/kg in core material containing visually abundant iron and manganese oxides on the surfaces of mineral grains adjacent to the screened interval of well MW-129S.

Graphical examination of elemental concentrations in geologic materials is used to identify materials of potential economic value as high concentrations depart from a log-normal data distribution (Sinclair, 1976; Rose and others, 1979; Risdianto and Kusnadi, 2010). Using this graphical approach, chromium concentrations in core material were distributed log-normally until an inflection point at about 85 mg/kg (fig. B.11*A*). This value is less than the average bulk continental abundance for chromium of 185 mg/kg (Reimann and de Caritat, 1998) and was used later in this professional paper as the summative-scale threshold value for chromium in core material used to evaluate high natural Cr(VI) concentrations in water from wells (chapter G). About 3 percent of core material adjacent to the screened interval of six sampled wells had higher chromium concentrations than expected from a log-normal distribution (table B.4). Sampled wells that have core material with chromium concentrations greater than 85 mg/kg included (1) MW-153S screened in weathered hornblende diorite bedrock in the western subarea, (2) MW-203D screened in Miocene deposits underlying unconsolidated material in the western subarea, (3) MW-186S3 screened in lake deposits containing basalt fragments in Water Valley, (4) MW-121D and MW-128S1 screened in Mojave-type deposits containing visually abundant secondary iron- and manganese-oxide coatings on the surfaces of mineral grains, and (5) MW-133S1 screened in fine-textured mudflat/playa deposits within the northern subarea (fig. B.6). Only weathered hornblende diorite bedrock adjacent to the screened interval of well MW-153S (fig. B.9) had chromium concentrations consistently greater than the summative-scale threshold of 85 mg/kg throughout the screened interval of the well. These data demonstrate that high-chromium concentrations in core material result from a number of different processes, which are not solely related to geologic source terrain. Although most high chromium concentrations are in silt or finer-textured material, oxide coatings on the surfaces of coarse-textured materials also provide additional surface-sorption sites for chromium and other trace elements, increasing their concentrations compared to host materials.

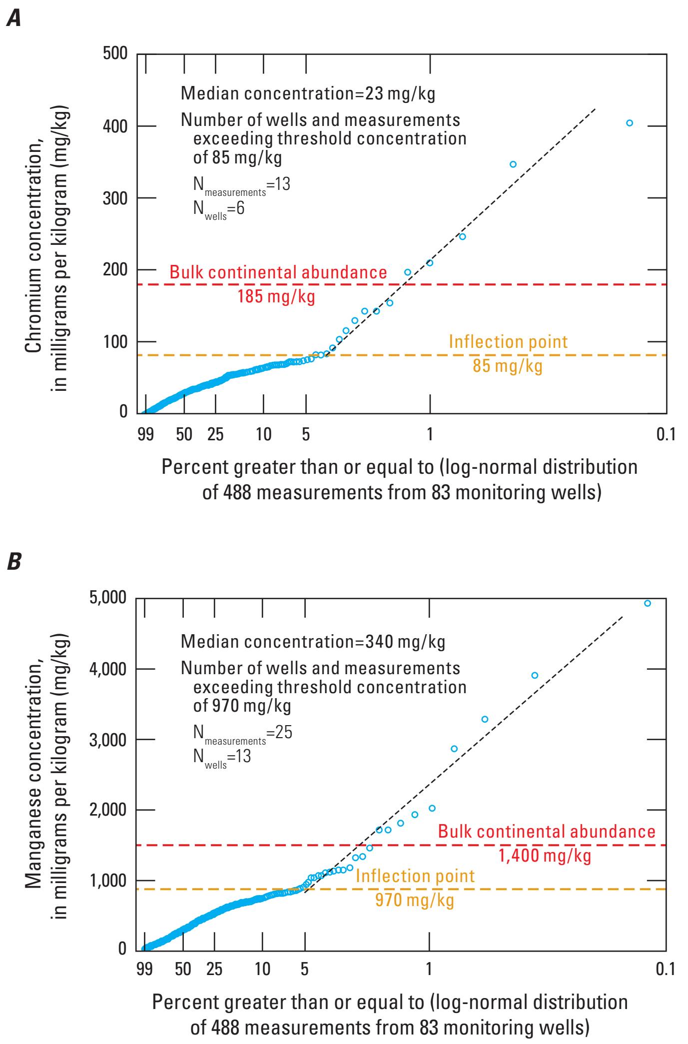

**Figure B.11.** Distribution of *A,* chromium and *B,* manganese in core material adjacent to the screened interval of sampled wells, Hinkley and Water Valleys, California. Data are available in Groover and Izbicki (2018).

## B.4.4. Manganese Concentrations in Core Material

In natural conditions, manganese oxides on the surfaces of mineral grains can oxidize Cr(III) to Cr(VI) (Schroeder and Lee, 1975). Manganese concentrations in core material adjacent to the screened interval of sampled wells in Hinkley and Water Valleys ranged from 28 to 4,930 mg/kg, with a median concentration of 340 mg/kg. Although manganese concentrations in core material are not discussed with the same level of detail as chromium, examination of data presented by Groover and Izbicki (2018) shows that manganese concentrations in core material within Hinkley and Water Valleys differ by subarea, depositional provenance, and texture in a manner similar to chromium. The oxidation state of manganese is not measured by pXRF but was evaluated on the basis of X-ray absorption near-edge structure (XANES; chapter C) and redox data (chapter E) later within this professional paper.

Similar to chromium, manganese concentrations in core material also were distributed log-normally until an inflection point at about 970 mg/kg (fig. B.11*B*). This value is less than the average bulk continental abundance for manganese of 1,400 mg/kg (Reimann and de Caritat, 1998) and was used later within this professional paper as the summative-scale threshold value for manganese in core material used to evaluate high natural Cr(VI) concentrations in water from wells (chapter G). About 5 percent of core material adjacent to the screened interval of 13 sampled wells (table B.4) have higher manganese concentrations than expected from a log-normal distribution. These wells include (1) MW-153S screened in weathered hornblende diorite bedrock in the western subarea, (2) MW-203D screened in Miocene deposits underlying unconsolidated material in the western subarea, (3) MW-136S2 and MW-154S1 in the northern subarea and MW-115S and BG-0004C in the eastern subarea screened in fine-textured mudflat/playa or lake deposits, and (4) BG-0004A, MW-121D, MW-128S1, and MW-186S3, which penetrate core material with visually abundant secondary iron- and manganese-oxide coatings on the surfaces of mineral grains (table B.4). Wells MW-153S, MW-121D, and MW-203D were previously identified as having chromium concentrations greater than the SSA threshold value of 85 mg/kg. Core material collected from 72 to 77 ft below land surface (bls) adjacent to the screened interval of well MW-154S1, sieved to remove gravel greater than 2 millimeters in diameter prior to mineralogic analyses (chapter C), also had chromium concentrations greater than the threshold value of 85 mg/kg.

**Table B.4.** Chromium and manganese concentrations in core material adjacent to the screened interval of sampled wells that equal or exceed threshold concentrations for summative-scale analysis, Hinkley and Water Valleys, California.

[Measurements made using portable (handheld) X-ray fluorescence (pXRF) in Groover and Izbicki (2018). Concentration is bold if it exceeds threshold chromium or manganese concentration. Depth to water data reported by Pacific Gas and Electric Company (PG&E) for MW-series wells. Depth to water data for BG-series wells measured by U.S. Geological Survey field personnel in January 2016. **Abbreviations**: blsd, below land surface datum; Q4 2015, fourth quarter, October–December 2015; mg/kg, milligram per kilogram; —, not applicable]

| Well | Screened interval (feet blsd) | Depth to water (feet blsd; Q4 2015) | Chromium | | | Manganese | | | Texture of chromium or manganese containing material | Provenance of material exceeding chromium or manganese threshold concentration | Visually abundant iron- and manganese-oxide coatings present |
|---|---|---|---|---|---|---|---|---|---|---|---|
| | | | Maximum within screened interval (mg/kg) | Median within screened interval (mg/kg) | Number of samples exceeding threshold concentration of 85 mg/kg | Maximum within screened interval (mg/kg) | Median within screened interval (mg/kg) | Number of samples exceeding threshold concentration of 970 mg/kg | | | |
| BG-0004A | 57–67 | 49.17 | 36 | 12 | 0 | **1,070** | 170 | 1 | Sand with fines | Mojave River | yes |
| BG-0004C | 155–165 | 61.51 | 60 | 38 | 0 | **1,780** | 850 | 4 | Silt or finer | Mudflat/playa | — |
| BG-0005B | 172–182 | 105.06 | 40 | 22 | 0 | **1,720** | 380 | 1 | Sand or coarser | Mojave River | — |
| MW-97S | 80–95 | 84.83 | 70 | 23 | 0 | **1,930** | 341 | 1 | Silt or finer | Lake margin | — |
| MW-115S | 75–90 | 65.22 | 66 | 56 | 0 | **1,189** | 640 | 1 | Silt or finer | Mudflat/playa | — |
| MW-119S | 75–90 | 76.74 | 69 | 26 | 0 | **3,280** | 460 | 3 | Silt or finer | Lake margin | — |
| MW-121D | 109–119 | 93.2 | **120** | 70 | 1 | **1,040** | 550 | 1 | Silt or finer | Lake margin | yes |
| MW-128S1 | 82–97 | 77.11 | **94** | 39 | 1 | 630 | 610 | 0 | sand | Mojave River | Yes |
| MW-131S1 | 68–83 | 67.83 | 68 | 50 | 0 | **3,900** | **1,120** | 3 | Rock fragments | Local fan | — |
| MW-133S | 65–80 | 70.1 | **85** | 36 | 1 | 840 | 520 | 0 | Silt or finer | Mudflat/playa | — |
| MW-136S2 | 117–127 | 75.25 | 66 | 34 | 0 | **1,130** | 530 | 2 | Silt or finer | Mudflat/playa | — |
| MW-153S | 93–108 | 91.3 | **405** | **130** | 5 | **4,940** | 690 | 3 | Saprolite | Weathered bedrock | — |
| [1]MW-154S1 | 70–85 | 68.9 | 77 | 70 | 0 | **1,340** | 830 | 3 | Silt or finer | Mudflat/playa | — |
| MW-158S | 100–115 | 101.9 | 58 | 40 | 0 | **1,710** | 480 | 1 | Silt or finer | Lake margin | — |
| MW-186S3 | 124–134 | 91.76 | **155** | 56 | 3 | 880 | 660 | 0 | Silt or finer | Lake deposits / basalt fragments | yes |
| MW-203D | 108–118 | 70.27 | **350** | 35 | 2 | **1,150** | 300 | 1 | Silt or finer | Local fan | — |

[1] Sieved core material collected for detailed mineralogy analyses from MW-154S1 at 72–77 feet blsd had chromium and manganese concentrations above threshold concentrations.

Chromium and manganese in core material from sampled wells are correlated with an $R^2=0.61$ (fig. B.12). Core material with more chromium than expected on the basis of its manganese concentration plots above the 95-percent predictive interval around the least-squares regression line through the data and includes material from wells MW-203D (in Miocene deposits), MW-153S (in weathered hornblende diorite), and MW-186S3 (in lake deposits containing basaltic fragments and visually abundant iron- and manganese-oxide coatings on the surfaces of mineral grains) that exceed the summative-scale threshold for chromium of 85 mg/kg (Groover and Izbicki, 2018). Core material from well BG-0005A completed in older Mojave River deposits had more chromium than expected on the basis of manganese concentrations in core material but did not exceed the SSA threshold of 85 mg/kg. Core material with less chromium than expected on the basis of its manganese concentration plots below the lower 95-percent predictive interval around the least-squares regression line and includes material from wells MW-131S1 containing accumulations of calcite associated with local geology, MW-119S in calcite-rich groundwater-discharge deposits, and BG-0005B and BG-0006A completed in caliche containing material (Groover and Izbicki, 2018). Core material from well MW-208S also plots below the lower 95-percent predictive interval around the least-squares regression line. Well MW-208S is within the October–December 2015 (Q4 2015) regulatory Cr(VI) plume and had a Cr(VI) concentration of 2,500 µg/L, the highest concentration sampled as part of this study. The chromium and manganese composition of core material from well MW-208S may be consistent with alteration of aquifer materials by high concentrations of Cr(VI), a strong oxidant, within the regulatory Cr(VI) plume.

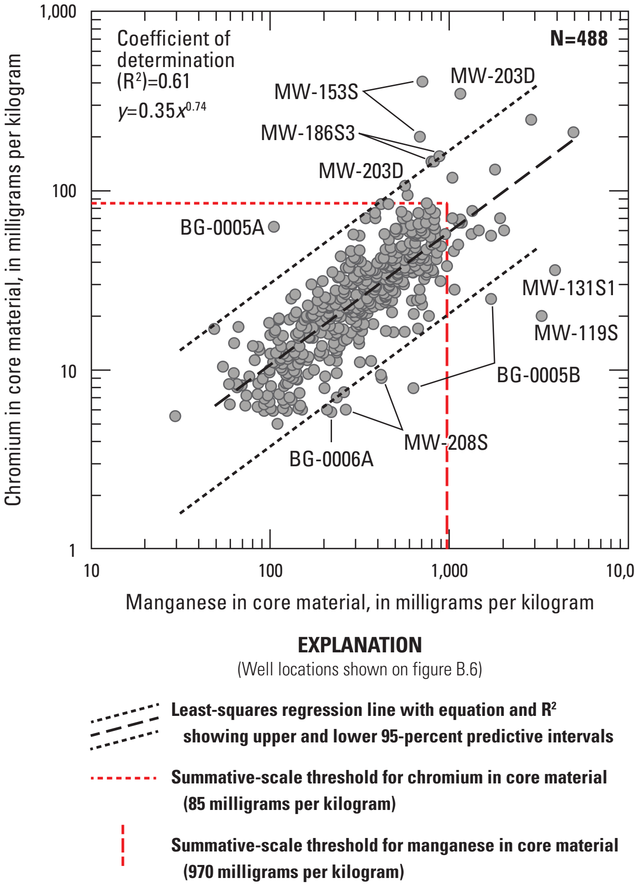

**Figure B.12.** Chromium as a function of manganese in core material adjacent to the screened interval of sampled wells, Hinkley and Water Valleys, California. Data are available in Groover and Izbicki (2018).

High chromium and high manganese concentrations in core material result from a number of different processes related to geologic source terrain and mineralogy. Most chromium and manganese concentrations greater than the SSA thresholds were present in silt or finer-textured material, and high concentrations were only present in coarse-sand textured Mojave River alluvium where visible accumulations of secondary iron- and manganese-oxide coatings on mineral grains were present. Mineralogy and weathering of minerals within aquifer materials is discussed in greater detail in chapter C within this professional paper.

## B.5. Elemental Assemblages in Surficial Alluvium, Rock, and Core Material

Principal component analysis was done to confirm interpretations of the occurrence of chromium within selected geologic source terrains within Hinkley and Water Valleys and to identify trace-element assemblages characteristic of those terrains. First, trace-element assemblages characteristic of selected geologic source terrains were identified using pXRF data from surficial alluvium. Second, these assemblages were confirmed using pXRF data from rock. Third, characteristic trace-element assemblages were used to identify the geologic source of material adjacent to the screened interval of sampled wells that may be difficult to identify solely on the basis of physical examination of core material. Trace-element assemblages that differ from the expected composition of the primary provenance were used evaluate the presence of admixtures of material eroded from local sources to core material adjacent to the screened interval of sampled wells. Finally, principal component scores were compared to data from wells elsewhere in the Mojave River groundwater basin to determine if chromium and concentrations of other elements in Hinkley and Water Valleys are in some way unique and differ from elemental assemblages present in nearby areas.

## B.5.1. Elemental Assemblages in Surficial Alluvium

Portable (handheld) X-ray fluorescence data include 179 measurements from more than 55 samples of surficial alluvium collected from alluviated stream channels, locally derived alluvial fan material, and Mojave River alluvium. Chromium in surficial alluvium was positively correlated with mafic elements including titanium, copper, manganese, and iron, with the largest magnitude Kendall's Tau β correlation coefficient (Kendall, 1938; Helsel and others, 2020) of 0.75 between chromium and iron (fig. B.13). The association of chromium with mafic elements is consistent with higher concentrations of chromium in older Mojave River alluvium containing mafic Pelona Schist eroded from the San Gabriel Mountains and with chromium in surficial alluvium eroded from hornblende diorite that crops out on Iron Mountain. Chromium and nickel commonly co-occur in mafic material and have similar PCA eigenvectors but have a comparatively low correlation coefficient of 0.22 (fig. B.13). Chromium in surficial alluvium is inversely correlated with the felsic elements, potassium and rubidium, consistent with low concentrations of chromium in recent Mojave River alluvium and higher chromium concentrations in older Mojave River alluvium, which contains some mafic alluvium eroded from the San Gabriel Mountains. Eigenvectors for potassium and rubidium are similar to eigenvectors for uranium. Uranium is present in felsic rock in the San Bernardino Mountains (U.S. Geological Survey, 2004; Smith and others, 2014; Groover and Izbicki, 2019).

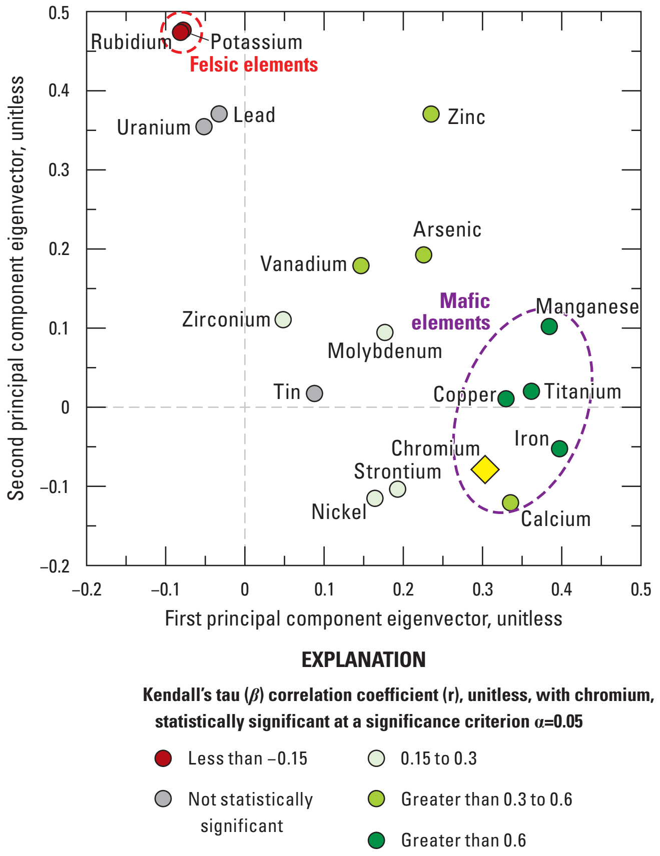

**Figure B.13.** First and second principal component analysis eigenvectors for surficial alluvium, Hinkley and Water Valleys, western Mojave Desert, California. Statistics were calculated from data available in Groover and Izbicki (2018).

Most first and second principal component scores for surficial alluvium were grouped near zero with a range of −3 to 3 along the x-axis (first principal component) and a range of −2 to 1 along the y-axis (second principal component; fig. B.14*A*). Samples of Mojave River alluvium generally fall within this body of data. Alluvium from the active channel of the Mojave River has a highly felsic composition, defined by more negative first principal component scores. Most chromium concentrations are generally less than the SRL of 5 mg/kg (fig. B.14*A*). Outside this body of data, principal component scores were distributed within three groups having different elemental assemblages representing different geologic source terrains.

The first group of data (fig. B.14*B*) has large magnitude positive first principal component scores and small magnitude negative second principal component scores. Large magnitude first principal component scores result from positive first PCA eigenvectors for calcium, iron, and chromium and other elements listed in table B.4. Higher concentrations of those elements are commonly associated with mafic terrain (Reimann and de Caritat, 1998). Negative second principal component scores result from lower concentrations of potassium and rubidium. Samples eroded from intrusive mafic rock (such as hornblende diorite and diorite) and mafic metamorphic rock (such as gneiss) that crop out on Iron Mountain are within this group (fig. B.14*B*). Chromium concentrations within this group generally increase as the elemental assemblages within alluvium becomes increasingly mafic (fig. B.14*B*). The ten highest chromium concentrations, and 17 of 23 samples of surficial alluvium with chromium concentrations greater than 50 mg/kg, were in surficial alluvium eroded from Iron Mountain.

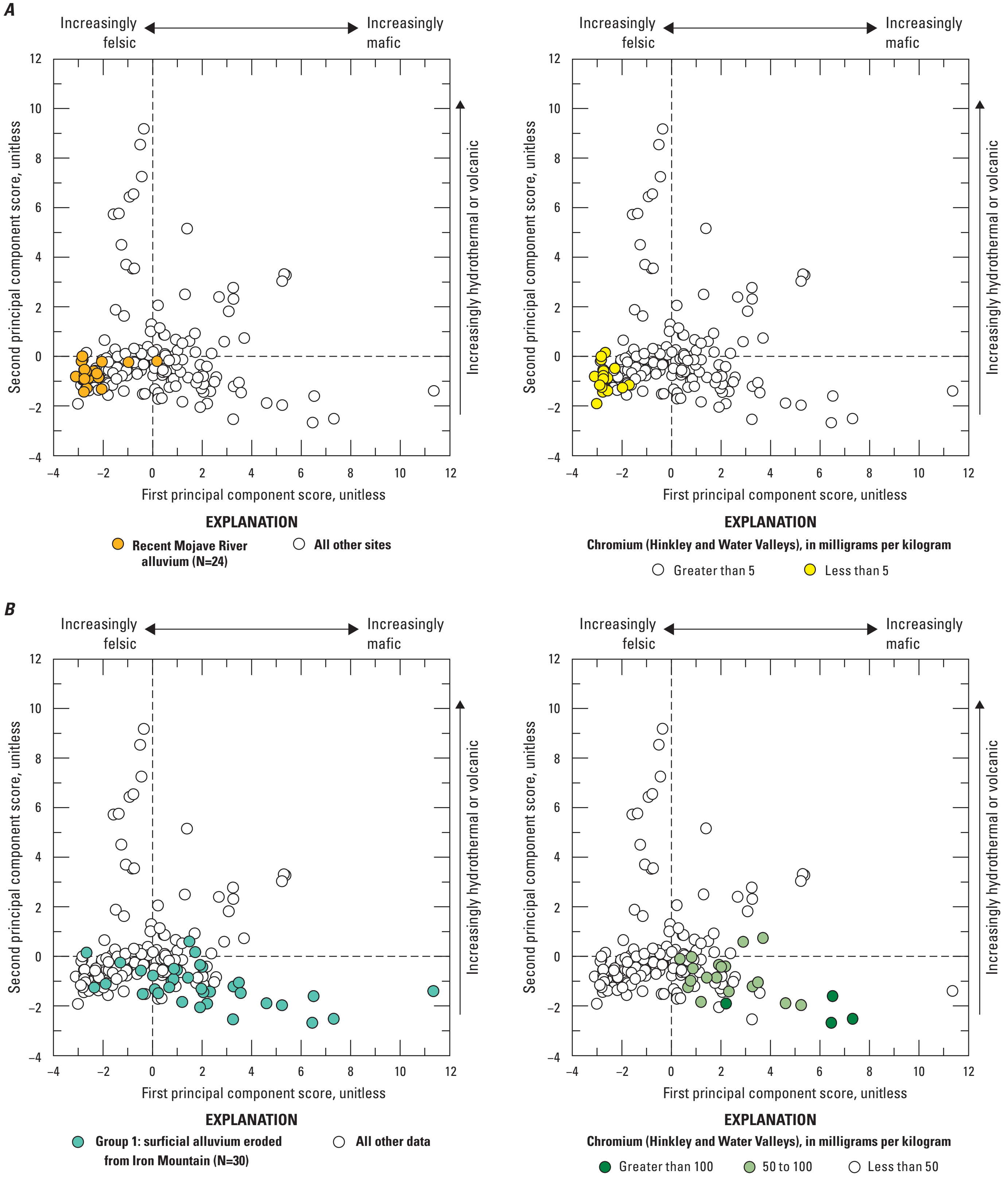

**Figure B.14.** First and second principal component scores for surficial alluvium eroded from selected source terrains, showing comparisons with *A,* surficial Mojave River alluvium and chromium concentrations, *B,* surficial alluvium eroded from Iron Mountain and chromium concentrations, and *C,* surficial alluvium eroded from Mount General and uranium concentrations, Hinkley and Water Valleys, western Mojave Desert, California. Statistics were calculated from data available in Groover and Izbicki (2018).

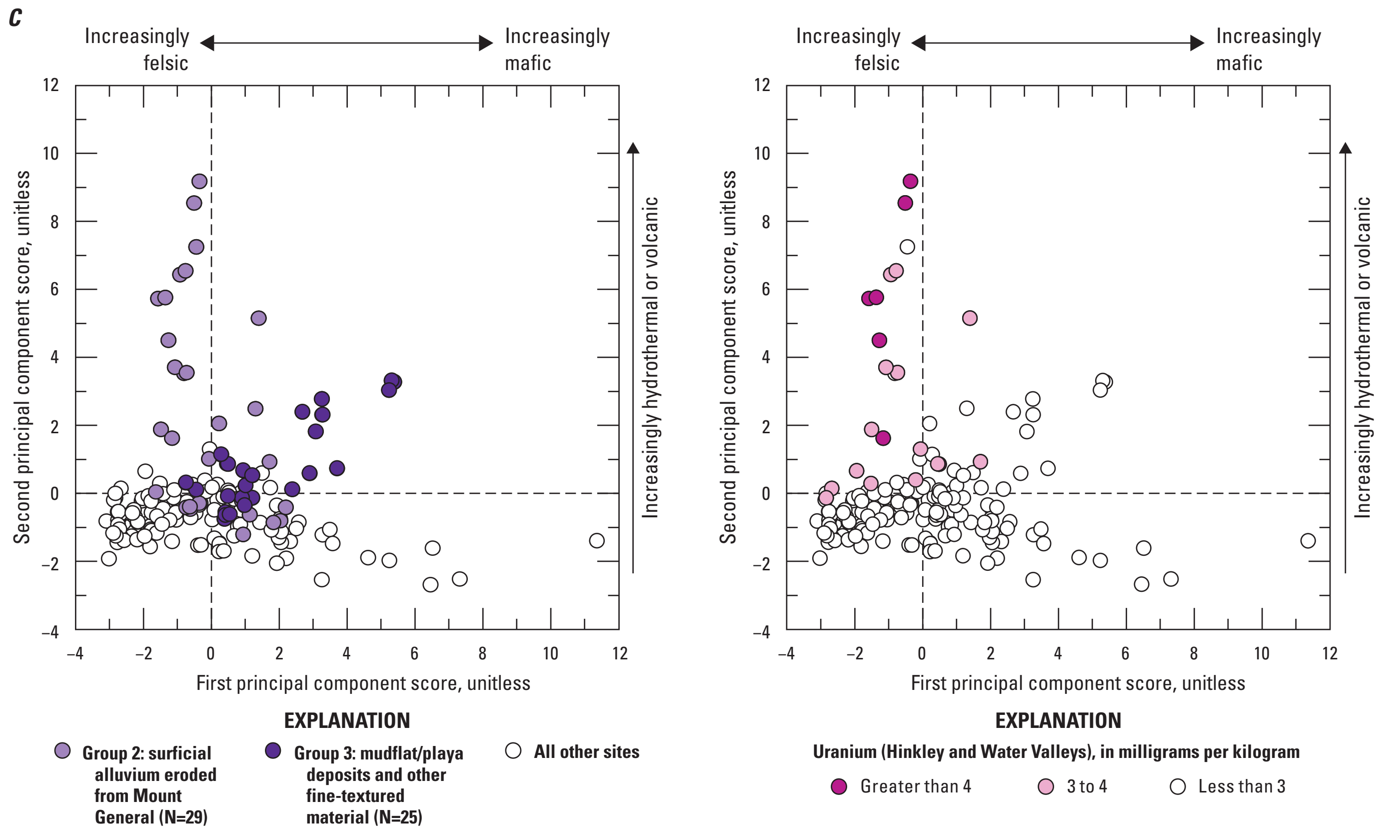

**Figure B.14.**—Continued

The second group of data (fig. B.14*C*) has large magnitude second principal component scores. These large magnitude scores reflect positive second principal component eigenvectors for rubidium, potassium, uranium, and lead (table B.5). Higher concentrations of those elements are commonly associated with felsic terrain, but also are associated with hydrothermal or volcanic terrains (Reimann and de Caritat, 1998; Housley and Reynolds, 2002). Samples eroded in part from hydrothermal and volcanic rock (such as rhyolite and dacite) that crop out on Mount General define this group (fig. B.14*C*). Uranium concentrations within this group generally increase as second principal component scores increase, with 7 of the 10 highest uranium concentrations in surficial alluvium eroded from Mount General (fig. B.14*C*). Chromium concentrations in surficial alluvium eroded from Mount General are not high, except in alluvium eroded from intrusive mafic (hornblende diorite) rock on the southern end of Mount General. As previously discussed, in recent geologic time much of this material would have been transported to areas outside Hinkley Valley by the Mojave River.

The third group of data (fig. B.14*C*) has large magnitude first and second principal component scores. Concentrations of most trace elements are higher than concentrations in recent Mojave River alluvium and generally increase within this group as first and second principal component scores increase. Increases in elemental concentrations are consistent with finer texture, greater surface area, and greater sorption of trace elements on oxide coatings on the surfaces of mineral grains within fine-textured deposits (Groover and Izbicki, 2019). Samples from fine-textured mudflat/playa deposits and other fine-textured alluvial deposits (such as mud sampled along alluviated stream channels) define this group (fig. B.14*C*). However, most chromium concentrations in surficial mudflat/playa deposits were less than 50 mg/kg, with the highest concentration of 52 mg/kg, and most uranium concentrations were less than the study reporting limit of 1.2 mg/kg. Mudflat/playa and fine-textured deposits in Hinkley and Water Valleys are largely sourced from the Mojave River; their felsic elemental composition differs from the mafic composition of fine-textured material in the northern subarea and within playa deposits eroded from mafic terrain elsewhere in the Mojave Desert, such as El Mirage (dry) Lake (Groover and Izbicki, 2019; fig. B.2), which has chromium concentrations as high as 490 mg/kg (not shown on fig. B.14*C*).

As previously discussed, most stream channels draining basaltic terrain are not alluviated and contain largely aeolian material from Harper (dry) Lake. These materials have a felsic composition typical of Mojave-type-deposits, and surficial alluvium eroded from basaltic volcanic terrain in the Water Valley area is not well-represented by PCA scores calculated from surficial alluvium.

**Table B.5.** Mean concentration, standard deviation, first, second, and third eigenvectors for selected elements from principal component analyses (PCA) of alluvium from known source terrains, Hinkley and Water Valleys, California.

[Mean, standard deviation, and eigenvectors calculated from portable X-ray fluorescence (pXRF) data for surficial alluvium eroded from known source areas in Groover and Izbicki (2018). Range in bulk continental abundance for selected elements from Nriagu and Nieboer (1988) and Reimann and de Caritat (1998). **Abbreviations**: mg/kg, milligram per kilogram; —, not applicable]

| Element[1] | Symbol | Mean (mg/kg) | Standard deviation (mg/kg) | Bulk continental abundance (mg/kg) | Loading on first eigenvector (unitless) | Loading on second eigenvector (unitless) | Difference between loadings on the first and second eigenvectors (unitless) |
|---|---|---|---|---|---|---|---|
| Elements associated with mafic source terrains | | | | | | | |
| Calcium | Ca | 31,900 | 25,500 | 38,500–52,900 | 0.33546 | −0.12106 | 0.45652 |
| Iron | Fe | 18,900 | 15,600 | 43,200–70,700 | 0.39743 | −0.05264 | 0.45007 |
| Chromium | Cr | 28.2 | 33.7 | 126–185 | 0.30335 | −0.07887 | 0.38221 |
| Titanium | Ti | 2,160 | 1,380 | 4,010–5,400 | 0.36199 | 0.01987 | 0.34212 |
| Copper | Cu | 14.8 | 14.5 | 25–75 | 0.32978 | 0.01050 | 0.31927 |
| Strontium | Sr | 458 | 173 | 260−330 | 0.19303 | −0.10374 | 0.29677 |
| Manganese | Mn | 351 | 234 | 720–1,400 | 0.38441 | 0.10181 | 0.28260 |
| Nickel | Ni | 28.7 | 12.2 | 56–105 | 0.16433 | −0.11539 | 0.27972 |
| Elements not strongly associated with a particular source terrains | | | | | | | |
| Molybdenum | Mo | 1.3 | 1.0 | 1–1.2 | 0.17699 | 0.09416 | 0.08283 |
| Tin | Sn | 12.5 | 6.7 | 2.3–2.5 | 0.08810 | 0.01703 | 0.07107 |
| Arsenic | As | 7 | 7.2 | 1–1.8 | 0.22587 | 0.19234 | 0.03353 |
| Vanadium | V | 113 | 222 | 98–230 | 0.14674 | 0.17874 | −0.03200 |
| Zirconium | Zr | 175 | 115 | 100–203 | 0.04840 | 0.11038 | −0.06197 |
| Zinc | Zn | 38.2 | 27.5 | 65–80 | 0.23532 | 0.37026 | −0.13495 |
| Elements associated with felsic, hydrothermal, or volcanic source terrains | | | | | | | |
| Lead | Pb | 16.5 | 13.9 | 8–14.8 | −0.03230 | 0.37054 | −0.40284 |
| Uranium | U | 1.8 | 0.8 | 0.91–2.7 | −0.05152 | 0.35439 | −0.40591 |
| Potassium | K | 26,200 | 11,500 | 9,100–21,400 | −0.07773 | 0.47629 | −0.55402 |
| Rubidium | Rb | 111 | 55.3 | 32–90 | −0.08111 | 0.47359 | −0.55471 |
| Proportion of variance explained (percent of total) | | | | | 29 | 21 | — |
| Cumulative variance explained (percent of total) | | | | | 29 | 50 | — |

[1] Elements ranked by difference between first and second principal components. Elemental data are from Groover and Izbicki (2018).

## B.5.2. Elemental Assemblages in Rock

Almost 200 pXRF measurements on more than 60 samples of rock (fig. B.3) collected in and near Hinkley and Water Valleys were used to evaluate performance of PCA results from surficial alluvium (fig. B.15). Rock data were not included within the PCA; instead, principal component scores for rock were calculated from eigenvectors estimated using PCA from surficial alluvium data (table B.1) using equation B.1. As expected, principal component scores calculated for rock in Hinkley and Water Valleys have greater magnitude and greater range (fig. B.14) than scores for alluvium eroded from source terrains containing those rocks (note scale differences between figures B.14 and B.15).

The general pattern and distribution of principal component scores calculated for rocks sampled from Iron Mountain (fig. B.15*A*; highly positive first principal component scores and smaller magnitude second principal component scores) is consistent with the composition of surficial alluvium eroded from that area (fig. B.14*B*). Intrusive basalts and mafic intrusive rock (hornblende diorite and diorite) from Iron Mountain have a similar mafic elemental assemblage, characterized by high magnitude positive first principal component scores, with the basalts having a more strongly mafic elemental assemblage than other mafic intrusive rock. Chromium concentrations generally increase with increasing first principal component scores for both rock types. Intrusive basalts have a limited areal extent within Iron Mountain, and although they have high chromium concentrations, they have limited impact on the elemental composition of alluvium eroded from Iron Mountain. The principal component scores for other rocks sampled from Iron Mountain range from felsic to mafic. Many rocks the crop out on Iron Mountain that have mafic elemental compositions have low chromium concentrations (fig. B.15*A*; table B.3).

In contrast to Iron Mountain, rocks from Mount General (fig. B.15*B*) have a wider range of elemental compositions than expected from PCA of surficial alluvium eroded from this area. Hydrothermal and some felsic volcanic rock from Mount General are highly mineralized, with high concentrations of arsenic, copper, lead, silver, uranium, vanadium, zinc, and other elements (Housley and Reynolds, 2002). Portable (handheld) X-ray fluorescence data show arsenic, lead, and uranium concentrations in hydrothermal rock from Mount General are as high as 1,700, 3,520, and 180 mg/kg, respectively. These mineralized rocks have high magnitude second principal component scores, occasionally greater than 1,000 (unitless; high values are not shown on fig. B.15*B*). Less mineralized hydrothermal and extrusive volcanic rocks (dacite and rhyolite) have high magnitude positive second principal component scores, similar to principal component scores in surficial alluvium. Mafic elemental compositions (large magnitude positive first principal component scores and negative second principal component scores) were calculated for pegmatite (not shown as a mappable unit on fig. B.3) that crops out within some intrusive felsic units on Mount General. Despite their mafic character, Mount General pegmatites have low chromium concentrations generally less than 5 mg/kg (Groover and Izbicki, 2018).

Felsic granitic rock from Lynx Cat Mountain is similar in elemental composition to alluvium eroded from felsic rock in the San Bernardino Mountains and transported to the area by the Mojave River (fig. B.15*C*). Alluvium eroded from granite composing Lynx Cat Mountain would be difficult to distinguish from Mojave River alluvium on the basis of its elemental composition. Basaltic rock within Water Valley has higher magnitude first and second principal component scores than Mojave River alluvium (fig. B.15*C*). Although calculated principal component scores for basalt are greater in magnitude, their elemental composition is similar to scores for some mudflat/playa deposits in the northern subarea. The median chromium concentrations for basaltic rock in Water Valley is 180 mg/kg with some concentrations as high as 310 mg/kg (table B.3).

## B.5.3. Elemental Assemblages in Core Material

Elemental assemblages and co-occurrence in core material from 490 pXRF measurements from sampled wells were examined on the basis of the first and second principal component scores. Scores for core material were calculated from eigenvectors for surficial alluvium in the same manner as rock data. The data were used to evaluate core material adjacent to well screens to identify (1) the geologic source of material adjacent to the screened interval of sampled wells that may be difficult to identify solely on the basis of physical examination of core material and (2) the presence of admixtures within core material eroded from different sources. In addition, the data also were used to identify the effect of secondary alteration of alluvium in groundwater-discharge areas and secondary alteration as a result of accumulation of iron- and manganese-oxide coatings on the surfaces of mineral grains near geologic, lithologic, and redox boundaries. As part of this exercise, pXRF data measured on core material in Hinkley and Water Valleys were compared with pXRF data measured on drill cuttings collected from wells elsewhere in the western Mojave Desert (Groover and Izbicki, 2018) to determine if concentrations of chromium and other elements in Hinkley and Water Valleys are in some way unique and differ from elemental assemblages present in nearby areas.

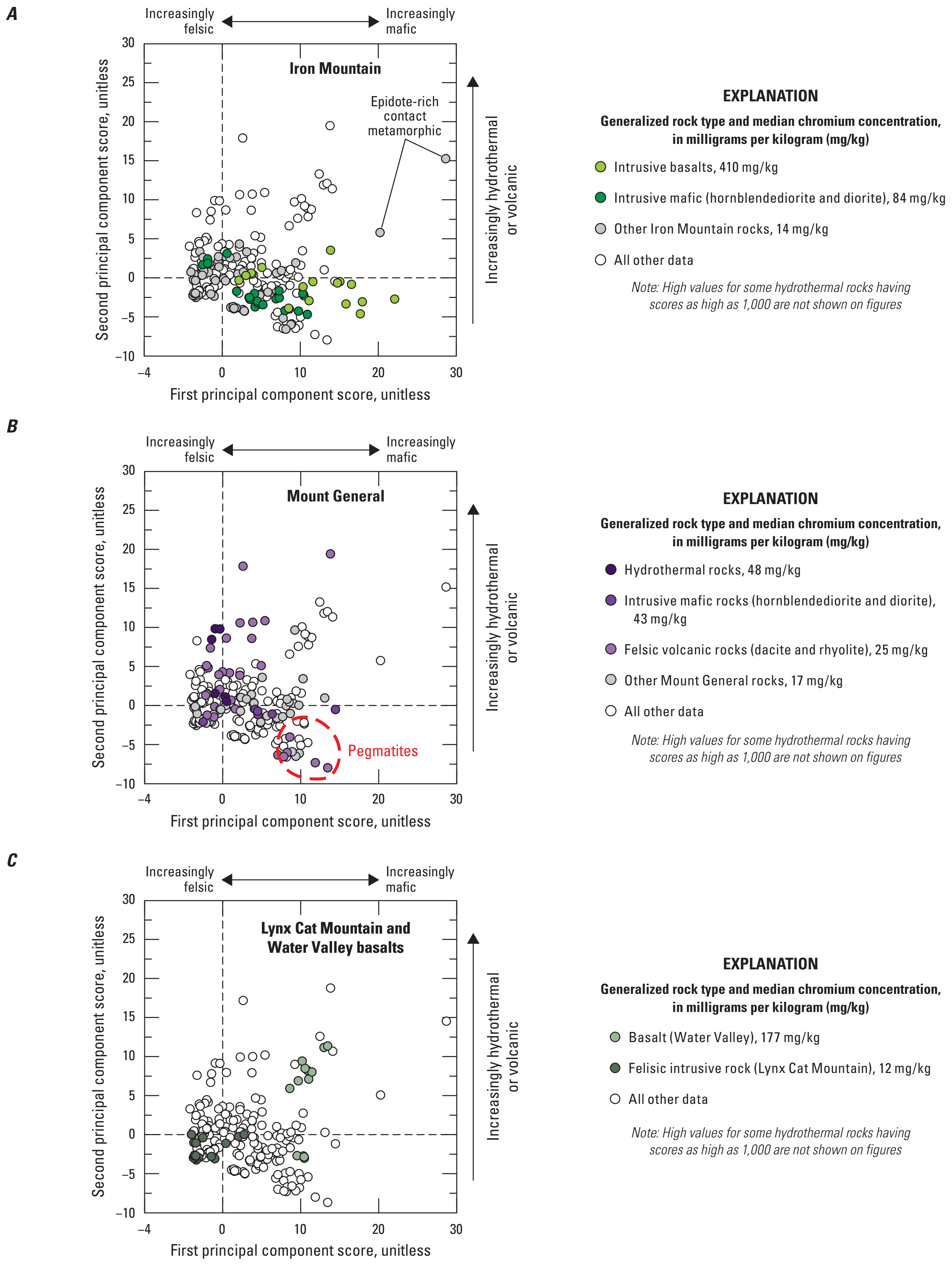

**Figure B.15.** First and second principal component scores for rock from *A,* Iron Mountain, *B,* Mount General, and *C,* Lynx Cat Mountain and Water Valley basalts, Hinkley and Water Valleys, California. Statistics were calculated from data available in Groover and Izbicki (2018).

The distribution and magnitude of calculated first and second principal component scores in core material was similar to the distribution of scores from surficial alluvium—with most values centered near zero and a felsic composition consistent with Mojave-type deposits eroded from the San Bernardino Mountains and deposited by the Mojave River (fig. B.16*A*). The elemental assemblage of Mojave River alluvium (unaltered by secondary processes) shifts from a highly felsic composition for sand and coarser-textured Mojave River materials to more positive first principal component scores in finer-textured material ultimately approaching the composition of mudflat/playa deposits (fig. B.16*A*). Sand-textured Mojave River core material adjacent to the screened interval of wells BG-0006B and MW-149S differs from similar texture Mojave River alluvium (fig. B.16*A*); this likely results from uranium concentrations in core material from those wells as high as 19 and 9.4 mg/kg, respectively. Uranium in core material from these wells was sourced from uranium-containing rock in the San Bernardino Mountains and transported to Hinkley Valley by the Mojave River and is not eroded from uranium-containing rock that crops out on Mount General.

Secondary alteration of unconsolidated aquifer material after deposition has produced distinct elemental compositions in core material adjacent to the screened interval of well MW-121D and to a lesser extent wells MW-163D and MW-128S1 (fig. B.16*B*). Alteration of these materials resulted in increased concentrations of most elements measured by pXRF and correspondingly higher first and second principal component scores compared to unaltered core material (fig. B.16*A*). Chromium concentrations in secondary iron and manganese oxides on core material from MW-121D are as high as 120 mg/kg (table B.4), several times greater than concentrations in similar textured unaltered core material. Similarly, arsenic concentrations in MW-121D exceeded 320 mg/kg in visually abundant iron- and manganese-oxide coatings on core material. For comparison, the average arsenic concentration in the bulk continental crust is 1 mg/kg (Reimann and de Caritat, 1998). In contrast, groundwater-discharge deposits, formed near the toe of alluvial lobes deposited when the ancestral Mojave River first entered Hinkley Valley (chapter A, fig. A.5; Miller and others, 2018, 2020), are characterized by calcite precipitates within Mojave River alluvium and near-shore lake deposits (fig. B.17). Groundwater-discharge deposits commonly have high first principal component scores and negative second principal component scores (fig. B.16*B*), but they are not mafic and not associated with high concentrations of chromium. However, uranium was present at concentrations greater than the reporting level of 2.0 mg/kg in 44 percent of groundwater-discharge deposits, and concentrations were as high as 19 mg/kg in calcite-rich groundwater-discharge deposits adjacent to well BG-0005B. Uranium in these materials originated from the Mojave River and felsic uranium-containing rock in the San Bernardino Mountains that accumulated to high concentrations as a result of secondary processes within the aquifer, rather than from uranium-containing rock in Mount General.

Principal component scores for weathered bedrock adjacent to the screened intervals of sampled wells have a wide range and indicate the composition of the original rock. For example, weathered hornblende diorite penetrated by wells MW-119D and MW-153S in the western subarea has mafic scores, while weathered granite penetrated by well MW-96S in the eastern subarea has felsic scores (fig. B.16*C*). The range of principal component scores for weathered bedrock is less than the range for rock values (fig. B.14). However, chromium concentrations in weathered rock are similar to the concentrations within the unweathered rock. Retention of chromium during weathering of hornblende diorite underlying aquifers in the western subarea of Hinkley Valley differs from the rapid removal of chromium during weathering of actinolite within soils developed on chromium-containing rock in the San Gabriel Mountains (Izbicki and others, 2008). This may result from differences in weathering processes in aquifer deposits within Hinkley and Water Valleys compared to pedogenesis (soil formation processes) in mountain areas that include leaching, or from differences in the types of chromium-containing minerals in the two areas (hornblende diorite in Hinkley Valley versus actinolite and fuchsite within the San Gabriel Mountains).

## B.5.4. Comparison with Regional Data

Portable (handheld) X-ray fluorescence data from core material adjacent to the screened intervals of wells in Hinkley and Water Valleys were compared to pXRF data measured on archived drill cuttings from 18 selected monitoring wells drilled by the USGS at sites in the Mojave River groundwater basin outside of Hinkley and Water Valleys (fig. B.2). The purpose of this comparison was to determine if core material from wells in Hinkley and Water Valleys was in some way unique or different from aquifer deposits in nearby areas.

The USGS monitoring wells selected for this comparison were drilled using mud-rotary techniques, and some wells were drilled to depths as great as 900 ft. Residual mud associated with drill cuttings did not affect pXRF data (Groover and Izbicki, 2018). Lithologic and geophysical logs from USGS monitoring wells are available from Huff and others (2002) and Izbicki and others (2000), and pXRF data from drill cuttings are available in Groover and Izbicki (2018). Drill cuttings from mud-rotary wells are physically mixed and averaged over 20-ft intervals by the drilling process. Consequently, the median PCA scores from core material adjacent to the screened interval of wells in Hinkley and Water Valleys, typically 10 ft, were used for comparison with drill cutting data. Principal component scores for drill cuttings were calculated using eigenvectors estimated from the PCA of surficial alluvium in the same manner as rock and core material from wells in Hinkley and Water Valleys.

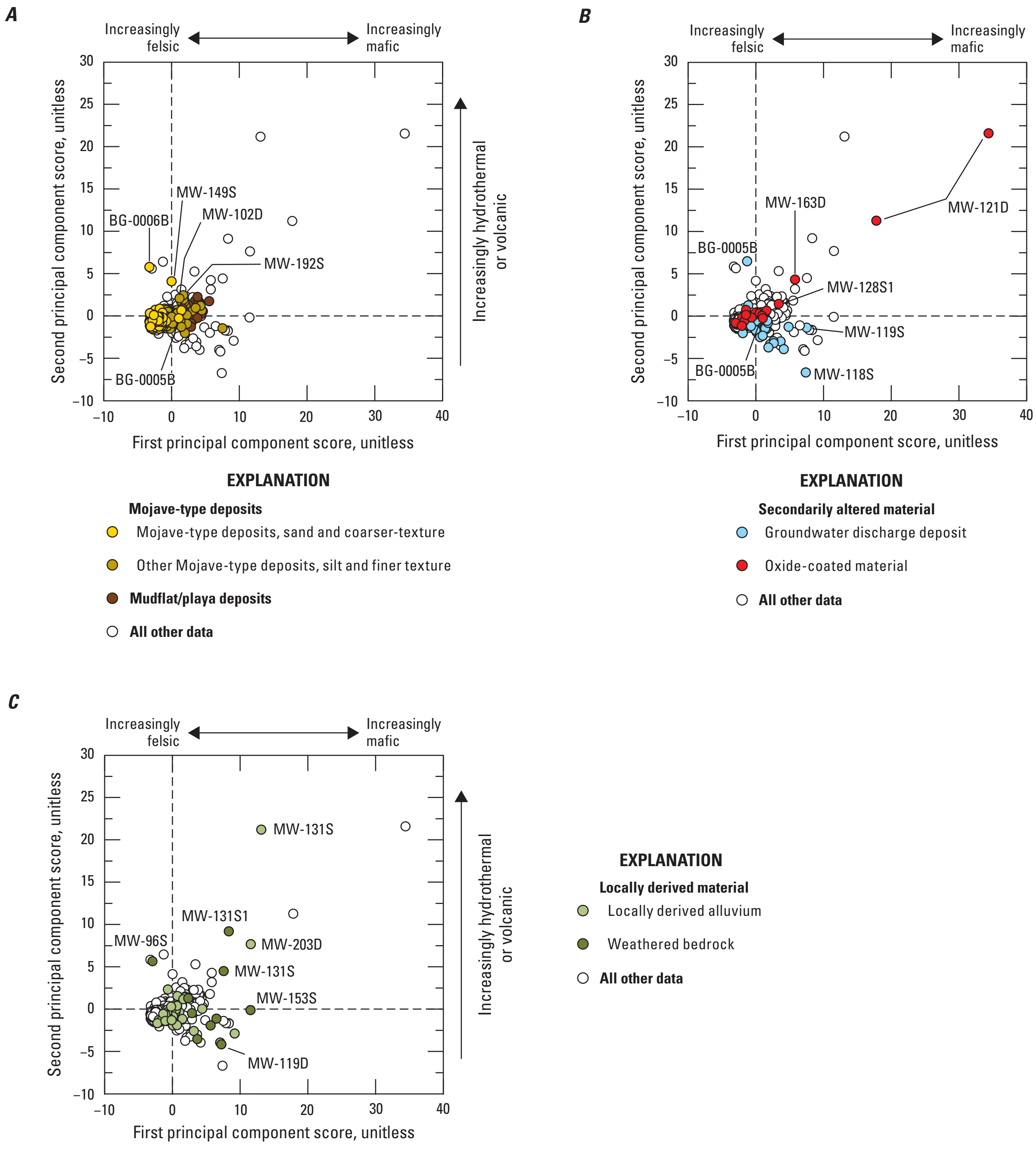

**Figure B.16.** First and second principal component scores for *A,* sand and finer-textured Mojave River deposits and mudflat/playa deposits, *B,* deposits having visually abundant secondary iron- and manganese-oxide coatings on mineral grains (various provenances and textures), and *C,* local alluvial fan deposits and weathered bedrock in core material adjacent to the screened interval of monitoring wells, Hinkley and Water Valleys, western Mojave Desert California. Statistics were calculated from data available in Groover and Izbicki (2018).

**Figure B.17.** Carbonate precipitates from ancestral groundwater-discharge deposits within core material adjacent to well MW-118S, western subarea, Hinkley Valley, western Mojave Desert, California. (Photograph by Krishangi Groover, U.S. Geological Survey, March 2016)

Calculated PCA scores from pXRF measurements for drill cuttings in the Mojave River groundwater basin show (1) a felsic composition for material within the floodplain aquifer along the Mojave River, (2) a mafic composition for material within the Sheep Creek fan eroded from mafic rock in the San Gabriel Mountains, and (3) a felsic volcanic and hydrothermal composition for alluvium and partly consolidated rock eroded from mountains north of Barstow (fig. B.18*A*). Admixtures of felsic volcanic and hydrothermal material were identified in the floodplain aquifer along the Mojave River downstream from Barstow but were not identified upstream from Barstow (fig. B.18*A*).

Median PCA scores for core material adjacent to the screened intervals of sampled wells in Hinkley and Water Valleys are similar to calculated scores for drill cuttings from wells elsewhere in the Mojave River groundwater basin. Data from Hinkley and Water Valleys do not appear to be different or unusual. The magnitude and range of data from Hinkley and Water Valleys are similar to data from the larger Mojave River groundwater basin, with most PCA scores for core material adjacent to the screened interval of wells in Hinkley and Water Valleys having a felsic composition consistent with a Mojave River origin (fig. B.18*B*). Although dry most of the time, the Mojave River near Barstow has recorded streamflows occasionally exceeding 64,000 cubic feet per second (ft$^3$/s; U.S. Geological Survey, 2021). The large quantity of material transported and deposited in Hinkley Valley by such large streamflows overwhelms smaller local sources that contribute alluvium to the valley.

Much of the data presentation and discussion in this chapter focuses on the composition of individual measurements of chromium concentrations and elemental composition of core material penetrated by wells. This was done to avoid obscuring high chromium values or unusual elemental compositions that may control aqueous chemistry. For example, wells MW-121D and MW-128S1 (not shown on fig. B.18*B*) have visually abundant iron- and manganese-oxide coatings on the surfaces of mineral grains and chromium concentrations that exceed the summative-scale threshold for chromium of 85 mg/kg (table B.4); however, when the entire interval penetrated by these wells is evaluated, the median PCA scores for these wells plot within the range of data for the floodplain aquifer.

In general, the median principal component scores and elemental assemblages of wells outside the felsic range of Mojave River materials are consistent with their lithology and depositional provenance (Groover and Izbicki, 2018; Miller and others 2020). Wells MW-119D and MW-153S, screened in weathered hornblende diorite underlying the western subarea within Hinkley Valley, have a mafic composition. Core material adjacent to the screened interval of well MW-186S3 in Water Valley contains basaltic fragments and has a mafic composition. The mafic compositions of core material from these wells are similar to the composition of drill cuttings from wells in the Sheep Creek fan eroded from mafic rock in the San Gabriel Mountains (fig. B.18*B*). Similarly, the median score for partly consolidated Miocene deposits penetrated by well MW-203D indicates the volcanic provenance of that material (Miller and others, 2020).

The median composition of core material adjacent to the screened interval of well MW-154S1 (fig. B.18*B*) in the northern subarea is consistent with the composition of mudflat/playa material (fig. B.16*B*). In contrast, the median composition of mudflat/playa deposits penetrated by nearby well MW-133S1 that have chromium concentrations greater than the threshold value of 85 mg/kg are within the range of floodplain aquifer compositions within the Mojave River groundwater basin (fig. B.18*A*). Core material adjacent to the screened intervals of wells MW-165D, MW-163D, and MW-155D are lacustrine (lake; chapter A, table A.1) deposits. Although water within these lakes may have been maintained by flow in the ancestral Mojave River (chapter A, fig. A.5), large volumes of Mojave River alluvium had not yet reached Hinkley Valley, and much of the lake sediment may have been locally derived. Core material from MW-131S1 has a composition representative of carbonate rock that crops out on Lynx Cat Mountain that is not well represented regionally in the Mojave River groundwater basin (fig. B.18*A*).

In contrast, median data from wells BG-0003A and MW-143S contain a greater mafic composition than expected on the basis of their Mojave-type depositional provenance (fig. B.16*B*). Despite their mafic composition, chromium concentrations in core material adjacent to the screened intervals of these wells did not exceed 13 and 26 mg/kg, respectively.

Comparison with regional data shows portable (handheld) X-ray fluorescence data measured on core material from wells in Hinkley and Water Valleys are not different or unusual compared to the magnitude and range of data from the larger Mojave River groundwater basin. Overall core material adjacent to the screened interval of most wells sampled for water chemistry and isotopic composition as part of this study have a low-chromium, felsic composition consistent with a Mojave River origin.

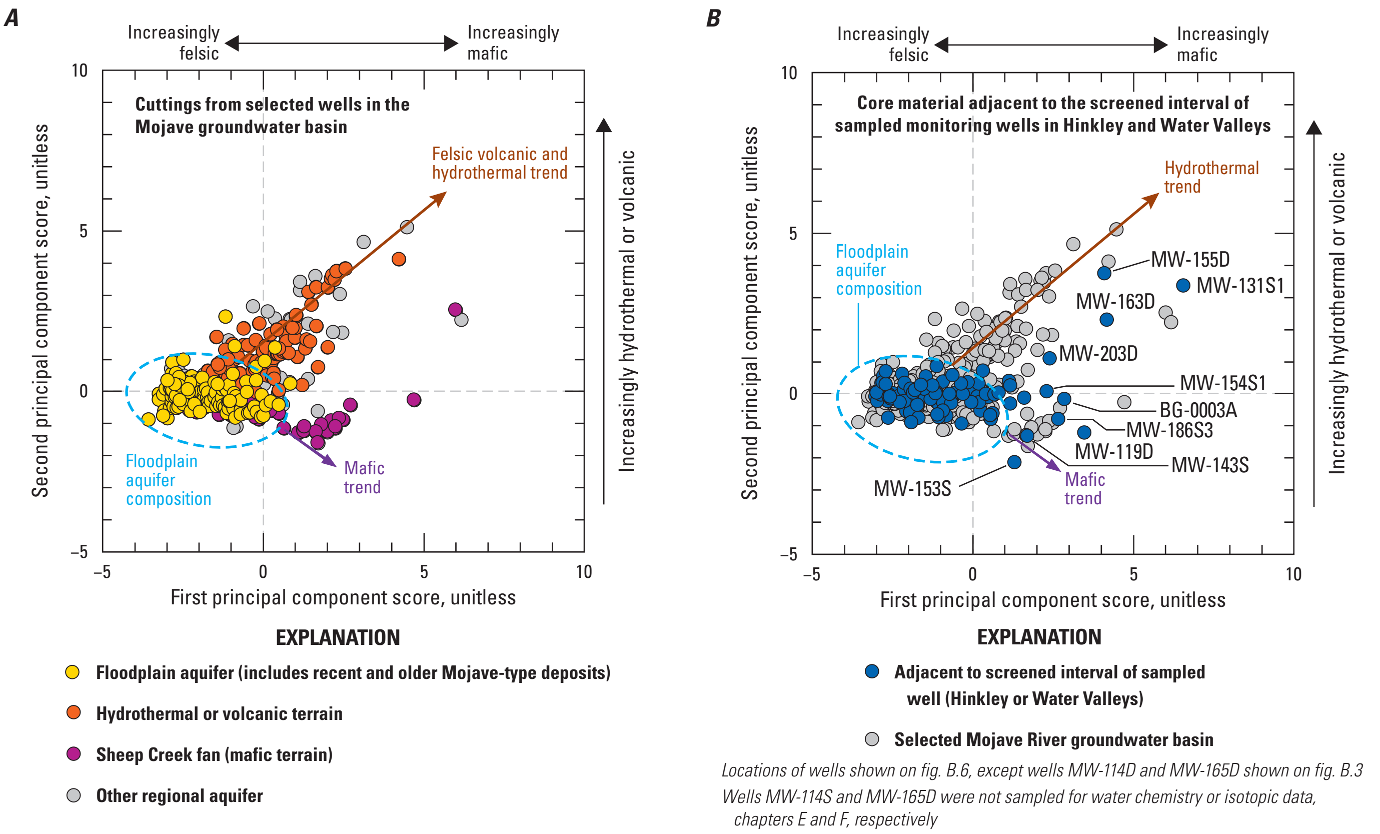

*Locations of wells shown on fig. B.6, except wells MW-114D and MW-165D shown on fig. B.3*

*Wells MW-114S and MW-165D were not sampled for water chemistry or isotopic data, chapters E and F, respectively*

**Figure B.18.** First and second principal component scores calculated from portable (handheld) X-ray fluorescence (pXRF) data for *A,* cuttings from selected U.S. Geological Survey monitoring wells in the Mojave River groundwater basin and *B,* core material adjacent to the screened interval of sampled wells in Hinkley and Water Valleys, western Mojave Desert, California. Statistics were calculated from data available in Groover and Izbicki (2018).

## B.6. Conclusions

Between 1952 and 1964, hexavalent chromium, Cr(VI), was released into groundwater from the Pacific Gas and Electric Company (PG&E) compressor station in Hinkley, California, in the western Mojave Desert 80 miles northeast of Los Angeles, California. In 2015, the extent of anthropogenic Cr(VI) in groundwater in Hinkley and Water Valleys was uncertain, and some Cr(VI) in groundwater may be naturally occurring from rock and aquifer material. The U.S. Geological Survey was requested by the Lahontan Regional Water Quality Control Board to complete an updated background study of Cr(VI) concentrations in Hinkley and Water Valleys.

On the basis of more than 1,500 portable (handheld) X-ray fluorescence (pXRF) measurements on more than 250 samples of rock, surficial alluvium, and core material, chromium concentrations in rock and surficial alluvium in most areas of Hinkley and Water Valleys are low compared to the average bulk continental abundance for chromium of 185 milligrams per kilogram (mg/kg). The median chromium concentrations in rock and surficial alluvium within Hinkley and Water Valleys were 26 and 22 mg/kg, respectively, and the median chromium concentration of surficial alluvium within the active channel of the Mojave River was less than 5 mg/kg. However, chromium concentrations are as high as 530 mg/kg in mafic intrusive rocks, including hornblende diorite, that crop out over 34 percent of the east slope of Iron Mountain draining toward the western subarea of Hinkley Valley. Additionally, chromium concentrations are as high as 310 mg/kg in basalt that crops out extensively in Water Valley. Local alluvium eroded from Iron Mountain has a median chromium concentration of 48 mg/kg, with concentrations as high as 295 mg/kg. In contrast, dacitic volcanic rocks that crop out on Mount General have a median chromium concentration of 28 mg/kg. Dacitic volcanic rocks do not contribute greatly to chromium occurrence in Hinkley Valley because of their low concentrations and admixtures of these materials do not result in measurable shifts in the elemental composition of core material. Although other high-chromium rocks are present elsewhere in Hinkley and Water Valleys, these rocks are either (1) not consistently high in chromium, (2) have limited areal extent, or (3) in the case of basalt, are primarily present in Water Valley.

Water from wells screened in unconsolidated materials that have higher chromium concentrations also may have higher Cr(VI) concentrations than wells screened in lower chromium material—assuming the pH, redox, and other aqueous geochemical properties that allow Cr(VI) to be present in groundwater are similar. Chromium concentrations in core material adjacent to the screen interval of sampled wells were log-normally distributed until an inflection point at about 85 mg/kg, with 3 percent of concentrations exceeding this value; this concentration was used as a metric (threshold value) to identify high natural chromium in core material. Chromium concentrations in core material from six sampled wells were greater than 85 mg/kg. These wells were identified as having high natural chromium in geologic material for the purposes of the summative-scale analysis (SSA) later in this professional paper (chapter G). Some of the higher chromium concentrations in core material result from chromium in local source rock, including weathered hornblende diorite bedrock associated with Iron Mountain and admixtures of locally derived alluvium with basalt in Water Valley. Bedrock associated with Iron Mountain underlies much of Hinkley Valley in the western and northern subarea, although bedrock knobs closest to the western excavation site are low in chromium. Chromium concentrations greater than 85 mg/kg also occur in fine-textured core material or result from processes that are not solely related to locally high geologic source terrain, including secondary oxidation of primary mineral grains and subsequent accumulation of iron- and manganese-oxide coatings on the surfaces of those grains. Secondary oxidation of mineral grains was observed near the water table and near geologic and lithologic contacts and chromium concentrations in visually abundant iron- and manganese-oxide coatings on the surfaces of mineral grains were as high as 120 mg/kg.

Manganese concentrations in core material are important to chromium occurrence in groundwater because of the role of manganese in the oxidation of trivalent chromium, Cr(III), to Cr(VI). Similar to chromium, manganese concentrations in core material were log-normally distributed until an inflection point at about 970 mg/kg, with 5 percent of concentrations exceeding this value. Manganese concentrations in core material from 13 sampled wells were greater than the threshold value of 970 mg/kg. Similar to chromium, high manganese concentrations in core material adjacent to sampled wells occur in fine-textured core material or result from accumulation of secondary manganese-oxide coatings on the surfaces of mineral grains.

Chromium and manganese concentrations in core material above threshold concentrations co-occur in several wells. Chromium and manganese concentrations were higher in silt or finer texture materials adjacent to the screened interval of sampled wells. Consequently, silt or finer texture also was used as a threshold metric for scoring within the SSA later in this professional paper (chapter G).

Arsenic concentrations in materials having visually abundant accumulations of secondary iron- and manganese-oxides can exceed 320 mg/kg; for comparison, the average bulk continental abundance of arsenic is 1 mg/kg. Secondary precipitation of calcite in groundwater-discharge deposits did not result in increased chromium concentrations above the host material. Chromium concentrations are commonly low in calcite-rich groundwater-discharge deposits buried within the aquifer. However, uranium concentrations in these materials are as high as 19 mg/kg; for comparison, the average bulk continental abundance of uranium is 0.9 mg/kg. Although Mount General is high in arsenic and uranium, high concentrations of these elements in groundwater within Hinkley and Water Valleys appear to be related to secondary alteration of Mojave-type deposits rather than to material eroded from Mount General.

Principal component analysis (PCA) was done on data for 18 elements measured in surficial alluvium, rock, and core material using pXRF. The PCA included evaluation of pXRF data from surficial alluvium, rock, and core material adjacent to the screened interval of sampled wells. Principal component analysis results showed distinct elemental compositions associated with (1) older and more recent felsic alluvium eroded from the San Bernardino Mountains, which was transported and deposited in the area by the Mojave River, (2) mafic rock and alluvium eroded from Iron Mountain, and (3) hydrothermal and volcanic rock, and alluvium eroded from Mount General. Playa and other fine-textured deposits in Hinkley and Water Valleys, and visually abundant secondary iron- and manganese-oxide coatings on the surfaces of mineral grains, also have identifiable compositions consistent with high concentrations of most elements measured by pXRF. Principal component analysis confirmed interpretations of the source of geologic materials that compose aquifers and the occurrence of chromium (and other elements) described on the basis of more traditional physical examination of geologic material including descriptions of texture and provenance done as part of this study.

The elemental composition of core material adjacent to wells sampled for water chemistry and isotopic composition as part of this study in Hinkley and Water Valleys spans a broad range that approximates the range in composition of core material from wells elsewhere in the Mojave River groundwater basin and western Mojave Desert. Most core material adjacent to the screened interval of sampled wells is composed of alluvium and near-shore, shallow lake deposits sourced from the Mojave River, referred to as Mojave-type deposits, and has a felsic, low-chromium composition. Shifts in the elemental composition of Mojave-type deposits associated with admixtures of local core material were identified in only a few wells on the basis of PCA of pXRF data. The absence of large shifts in elemental composition of core material attributable to admixtures from local source material is consistent with transport and deposition of large quantities of material by occasional large streamflows in the Mojave River, which overwhelms smaller local sources. Chromium concentrations in alluvium associated with dacitic rock eroded from Mount General are low, and alluvium that contains admixtures eroded from dacitic rock that crops out on Mount General do not contribute high concentrations of chromium to aquifer materials within the eastern subarea.

## B.7 References Cited

ARCADIS, 2016, Annual cleanup status and effectiveness report (January to December 2015) Pacific Gas and Electric Company, Hinkley Compressor Station, Hinkley, California: San Francisco, Calif., Pacific Gas and Electric Company, prepared by ARCADIS, Oakland, Calif., RC000699, [variously paged], accessed February 2016, at https://documents.geotracker.waterboards.ca.gov/esi/uploads/geo_report/9395357131/SL0607111288.PDF.

ARCADIS and CH2M Hill, 2011, Development of a groundwater flow and solute transport model, appendix G *of* Pacific Gas and Electric Company, Addendum #3 to the Hinkley Compressor Station site feasibility study: San Francisco, Calif., Pacific Gas and Electric Company, [variously paged], accessed March 5, 2019, at https://geotracker.waterboards.ca.gov/esi/uploads/geo_report/2112934887/SL0607111288.pdf.

Belitz, K., Dubrovsky, N.M., Burow, K., Jurgens, B.C., Johnson, T., 2003, Framework for a ground-water quality monitoring and assessment program for California: U.S. Geological Survey Water-Resources Investigations Report 2003–4166, 78 p., accessed December 2, 2020, at https://doi.org/10.3133/wri034166.

Boettcher, S.S., 1990, Geologic map of Iron Mountain: Geological Society of America Digital Map and Chart Series 19, 1:12,000 scale, https://doi.org/10.1130/1990-boettcher-ironmountain.

California Department of Water Resources, 2003, California's groundwater: Bulletin 118, 7 p., accessed November 20, 2018, at https://water.ca.gov/Programs/Groundwater-Management/Bulletin-118.

California Department of Water Resources, 2019, California's groundwater—Basin boundary modifications: California Department of Water Resources Bulletin 118, accessed June 12, 2019, at https://water.ca.gov/Programs/Groundwater-Management/Basin-Boundary-Modifications.

CH2M Hill, 2007, Groundwater background study report—Hinkley compressor station, Hinkley, California: San Francisco, Calif., Pacific Gas and Electric Company, prepared by CH2M Hill, Oakland, Calif., [variously paged], accessed January 12, 2018, at https://www.waterboards.ca.gov/lahontan/water_issues/projects/pge/docs/2007_background_study_report.pdf.

CH2M Hill, 2013, Conceptual site model for groundwater flow and the occurrence of chromium in groundwater of the western area, Pacific Gas and Electric Company, Hinkley Compressor Station, Hinkley, California: San Francisco, Calif., Pacific Gas and Electric Company, prepared by CH2M Hill, Oakland, Calif., [variously paged], accessed December 10, 2019, at https://geotracker.waterboards.ca.gov/esi/uploads/geo_report/7274906218/SL0607111288.pdf.

Chaffee, M.A., 1975, Geochemical exploration techniques applicable in the search for copper deposits: U.S. Geological Survey Professional Paper 907-B, 26 p., https://doi.org/10.3133/pp907B.

Cox, B.F., Hillhouse, J.W., and Owen, L.A., 2003, Pliocene and Pleistocene evolution of the Mojave River, and associated tectonic development of the Transverse Ranges and Mojave Desert, based on borehole stratigraphy studies and mapping of landforms and sediments near Victorville, California, *in* Enzel, Y., Wells, S.G., and Lancaster, N., eds., Paleoenvironments and paleohydrology of the Mojave and southern Great Basin deserts—Boulder, Colorado: Geological Society of America Special Paper 368, p. 1–42, https://doi.org/10.1130/0-8137-2368-X.1.

Dibblee, T.W., Jr., 1960a, Geologic map of the Barstow quadrangle, San Bernardino County, California: U.S. Geological Survey Mineral Investigations Field Studies Map MF-233, scale 1:62,500, accessed November 26, 2018, at https://doi.org/10.3133/mf233.

Dibblee, T.W., Jr., 1960b, Geologic map of the Hawes quadrangle, San Bernardino County, California: U.S. Geological Survey Mineral Investigations Field Studies Map MF-226, scale 1:62,500, accessed November 26, 2018, at https://doi.org/10.3133/mf226.

Emsley, J., 2001, Nature's building blocks—An A–Z guide to the elements: Oxford, U.K., Oxford University Press, 498 p.

Fletcher, J.M., Bartley, J.M., Martin, M.W., Glazner, A.F., and Walker, J.D., 1995, Large-magnitude continental extension—An example from the central Mojave metamorphic core complex: Geological Society of America Bulletin, v. 107, no. 12, p. 1468–1483, https://doi.org/10.1130/0016-7606(1995)107<1468:LMCEAE>2.3.CO;2.

Fletcher, J.M., Miller, J.S., Martin, M.W., Boettcher, S.S., Glazner, A.F., and Bartley, J.M., 2002, Cretaceous arc in the Mojave block—Profound crustal modification that controlled subsequent tectonic regimes, *in* Glazner, A.F., Walker, J.D., and Bartley, J.M., eds., Geologic evolution of the Mojave Desert and southwestern Basin and Range: Geological Society of America Memoir 195, p. 19–41, https://doi.org/10.1130/0-8137-1195-9.131.

Folk, R.L., 1954, The distinction between grain size and mineral composition in sedimentary-rock nomenclature: The Journal of Geology, v. 62, no. 4, p. 344–359, https://doi.org/10.1086/626171.

Gough, L.P., Severson, R.C., and Shacklette, H.T., 1988, Element concentrations in soils and other surficial materials of Alaska: U.S. Geological Survey Professional Paper 1458, 53 p., accessed August 2, 2017, at https://doi.org/10.3133/pp1458.

Gough, L.P., Wang, B., Smith, D.B., and Gustavsson, N., 2005, Geochemical landscapes of Alaska—New map presentations and interpretations for 23 elements in surficial materials: U.S. Geological Survey Professional Paper 1716, 36 p., accessed August 2, 2017, at https://doi.org/10.3133/pp1716.

Graham, G.E., Taylor, R.D., Lee, G.K., and Tripp, R.B., 2015, Targeting Cu-Au and Mo resources using multi-media exploration geochemistry—An example from Tyonek quadrangle, Alaska Range, Alaska: Journal of Geochemical Exploration, v. 157, p. 52–65, https://doi.org/10.1016/j.gexplo.2015.05.014.

Groover, K.D., 2016, Elemental analysis using a handheld X-ray fluorescence spectrometer: U.S. Geological Survey Fact Sheet 2016–3043, 2 p., accessed August 2, 2017, at https://doi.org/10.3133/fs20163043.

Groover, K.D., and Izbicki, J.A., 2018, Field portable X-ray fluorescence and associated quality control data for the western Mojave Desert, San Bernardino County, California: U.S. Geological Survey data release, accessed November 29, 2018, at https://doi.org/10.5066/P9CU0EH3.

Groover, K.D., and Izbicki, J.A., 2019, Selected trace-elements in alluvium and rocks, western Mojave Desert, southern California: Journal of Geochemical Exploration, v. 200, p. 234–248, accessed July 8, 2019, at https://doi.org/10.1016/j.gexplo.2018.09.005.

Grunsky, E.C., and de Caritat, P., 2019, State-of-the-art analysis of geochemical data for mineral exploration: Geological Society of London; Geochemistry, Exploration, Environment, and Analysis: Geological Society of London, v. 20, no. 2, p. 217–232, accessed July 23, 2019, at https://doi.org/10.1144/geochem2019-031.

Helsel, D.R., Hirsch, R.M., Ryberg, K.R., Archfield, S.A., and Gilroy, E.J., 2020, Statistical methods in water resources: U.S. Geological Survey Techniques and Methods, book 4, chap. A3, 458 p., accessed October 31, 2022, at https://doi.org/10.3133/tm4A3.

Housley, R.M., and Reynolds, R.E., 2002, Mineralogical survey of the Mount General area, *in* Reynolds, R.E., ed., Between the basins—Exploring the western Mojave and Basin and Range Province: 2002 Desert Symposium, p. 61–63, California State University, Fullerton, Desert Studies Consortium.

Hotelling, H., 1933, Analysis of a complex of statistical variables into principal components: Journal of Educational Psychology, v. 24, no. 6, p. 417–441, https://doi.org/10.1037/h0071325.

Huff, J.A., Clark, D.A., and Martin, P., 2002, Lithologic and ground-water data for monitoring sites in the Mojave River and Morongo ground-water basins, San Bernardino County, California, 1992–98, Appendix D: U.S. Geological Survey Open-File Report 2002–354, p. 181–294, accessed November 26, 2020, at https://doi.org/10.3133/ofr02354.

Izbicki, J.A., and Groover, K.D., 2016, A plan for study of natural and man-made hexavalent chromium, Cr(VI), in groundwater near a mapped plume, Hinkley, California: U.S. Geological Survey Open-File Report 2016–1004, 12 p., accessed November 28, 2018, at https://doi.org/10.3133/ofr20161004.

Izbicki, J.A., and Groover, K.D., 2018, Natural and man-made hexavalent chromium, Cr(VI), in groundwater near a mapped plume, Hinkley, California—Study progress as of May 2017, and a summative-scale approach to estimate background Cr(VI) concentrations: U.S. Geological Survey Open-File Report 2018–1045, 28 p., accessed November 28, 2018, at https://doi.org/10.3133/ofr20181045.

Izbicki, J.A., Clark, D.A., Pimental, M.I., Land, M., Radyk, J.C., and Michel, R.L., 2000, Data from a thick unsaturated zone underlying Oro Grande and Sheep Creek washes in the western part of the Mojave Desert, near Victorville, San Bernardino County, California: U.S. Geological Survey Open-File Report 2000–262, 133 p., accessed December 4, 2018, at https://doi.org/10.3133/ofr00262.

Izbicki, J.A., Ball, J.W., Bullen, T.D., and Sutley, S.J., 2008, Chromium, chromium isotopes and selected trace elements, western Mojave Desert, USA: Applied Geochemistry, v. 23, no. 5, p. 1325–1352, accessed September 10, 2018, at https://doi.org/10.1016/j.apgeochem.2007.11.015.

Jennings, C.W., with modifications by Gutierrez, C., Bryant, W., Saucedo, G., and Wills, C., 2010, Geologic map of California: California Geological Survey, Geologic Data Map No. 2, scale 1:750,000.

Kendall, M.G., 1938, A new measure of rank correlation: Biometrika, v. 30, no. 1–2, p. 81–93, accessed October 31, 2022, at https://doi.org/10.1093/biomet/30.1-2.81.

Kruckeberg, A.R., 1984, California serpentines—Flora, vegetation, geology, soils, and management problems: Berkeley, University of California Press, Ltd., 180 p.

Lahontan Regional Water Quality Control Board, 2008, Staff report—Background chromium study Pacific Gas and Electric Company Compressor Station: South Lake Tahoe, Calif., California Regional Water Quality Control Board, Lahontan Region, [variously paged], accessed November 20, 2018, at http://www.swrcb.ca.gov/rwqcb6/water_issues/projects/pge/docs/backgroundstudy_pge8_08.pdf.

Lahontan Regional Water Quality Control Board, 2014, Comments on report for cleanup of waste pit (western excavation site), Pacific Gas and Electric (PG&E), San Bernardino County (Assessor Parcel No. 0488-074-03), WDID NO., 6B361403001: California Water Boards Investigative Order No. R6V-2014-0019, accessed December 14, 2018, at https://www.waterboards.ca.gov/lahontan/board_decisions/adopted_orders/2014/docs/19.pdf.

Meisling, K.E., and Weldon, R.J., 1989, Late Cenozoic tectonics of the northwestern San Bernardino Mountains, southern California: Geological Society of America Bulletin, v. 101, no. 1, p. 106–128, https://doi.org/10.1130/0016-7606(1989)101<0106:LCTOTN>2.3.CO;2.

Miller, D.M., Haddon, E.K., Langenheim, V.E., Cyr, A.J., Wan, E., Walkup, L.C., and Starratt, S.W., 2018, Middle Pleistocene infill of Hinkley Valley by Mojave River sediment and associated lake sediment—Depositional architecture and deformation by strike-slip faults, *in* Miller, D.M., ed., The Mojave River from sink to source: The 2018 Desert Symposium Field Guide and Proceedings, April 2018, accessed November 27, 2018, at http://www.desertsymposium.org/2018%20DS%20Against%20the%20Current.pdf.

Miller, D.M., Langenheim, V.E., and Haddon, E.K., 2020, Geologic map and borehole stratigraphy of Hinkley Valley and vicinity, San Bernardino County, California: U.S. Geological Survey Scientific Investigations Map 3458, 23 p. pamphlet, 2 sheets, scale 1:24,000, https://doi.org/10.3133/sim3458.

Mojave Water Agency, 2014, Geospatial library, accessed May 22, 2014, at https://www.mojavewater.org/data-maps/geospatial-library/.

Morrison, J.M., Benzel, W.M., Holm-Denoma, C.S., and Bala, S., 2018, Grain size, mineralogic, and trace-element data from field samples near Hinkley, California: U.S. Geological Survey data release, accessed July 24, 2019, at https://doi.org/10.5066/P9HUPMG0.

Munsell Color, 1975, Munsell soil color charts: Baltimore, Md., Munsell Color, Inc.

Munsell Color, 1994, Munsell soil color charts: Baltimore, Md., Munsell Color, Inc.

National Institute of Standards and Technology, 2018, Certificate of analysis, standard reference material 2710a, Montana I soil, highly elevated trace element concentrations: Gaithersburg, Md., National Institute of Standards and Technology, 7 p., accessed October 31, 2022, at https://assets.lgcstandards.com/sys-master%2Fpdfs%2Fh37%2Fh13%2F10132333920286%2FCOA_NIST-2710A_ST-WB-CERT-2828053-1-1-1.PDF?_ga=2.199384684.353942319.1681083437-1310393241.1681083437.

National Institute of Standards and Technology, 2022, Certificate of analysis, standard reference material 2711a, Montana II soil, moderately elevated trace element concentrations: Gaithersburg, Md., National Institute of Standards and Technology, 8 p., accessed October 31, 2022, at https://assets.lgcstandards.com/sys-master%2Fpdfs%2Fh82%2Fhfc%2F10333739319326%2FCOA_NIST-2711A_ST-WB-CERT-3406664-1-1-1.PDF?_ga=2.266092237.353942319.1681083437-1310393241.1681083437.

National Research Council, 1947, Report of the subcommittee on sediment terminology: Eos, Transactions American Geophysical Union, v. 28, no. 6, p. 936–938, https://doi.org/10.1029/TR028i006p00936.

Neter, J., and Wasserman, W., 1974, Applied linear statistical models: Homewood, Ill., Richard D. Irwin Inc., 152 p.

Ninyo and Moore, 2009, Geotechnical evaluation, Mojave solar project, Lockhart, California, Appendix B—Geotechnical evaluation: San Diego, Calif., Ninyo and Moore Consultants, Project No. 1085790004, [variously paged].

Nriagu, J.O., and Nieboer, E., eds., 1988, Chromium in the natural and human environments: New York, John Wiley & Sons, 571 p.

Painter, S., Cameron, E.M., Allan, R., and Rouse, J., 1994, Reconnaissance geochemistry and its environmental relevance: Journal of Geochemical Exploration, v. 51, no. 3, p. 213–246, https://doi.org/10.1016/0375-6742(94)90008-6.

Reheis, M.C., Bright, J., Lund, S.P., Miller, D.M., Skipp, G., and Fleck, R.J., 2012, A half-million-year record of paleoclimate from the Lake Manix core, Mojave Desert, California: Palaeogeography, Palaeoclimatology, Palaeoecology, v. 365–366, p. 11–37, https://doi.org/10.1016/j.palaeo.2012.09.002.

Reimann, C., and de Caritat, P., 1998, Chemical elements in the environment: Berlin, Germany, Springer-Verlag, 398 p., https://doi.org/10.1007/978-3-642-72016-1.

Risdianto, D., and Kusnadi, D., 2010, The application of a probability graph in geothermal exploration: Proceedings World Geothermal Congress, Bali, Indonesia, 6 p.

Rose, A.W., Hawkes, H.E., and Webb, J.S., 1979, Geochemistry in mineral exploration: New York, Academic Press, 657 p.

Schroeder, D.C., and Lee, G.F., 1975, Potential transformations of chromium in natural waters: Water, Air, and Soil Pollution, v. 4, no. 3–4, p. 355–365, https://doi.org/10.1007/BF00280721.

Shacklette, H.T., and Boerngen, J.G., 1984, Element concentrations in soils and other surficial materials of the conterminous United States: U.S. Geological Survey Professional Paper 1270, 105 p., accessed August 2, 2017, at https://doi.org/10.3133/pp1270.

Shacklette, H.T., Hamilton, J.C., Boerngen, J.G., and Bowles, J.M., 1971, Elemental composition of surficial materials in the conterminous United States: U.S. Geological Survey Professional Paper 574–D, accessed August 2, 2017, at https://doi.org/10.3133/pp574D.

Sinclair, A.J., 1976, Applications of probability graphs in mineral exploration: The Association of Exploration Geochemists, Special Volume no. 4, 95 p.

Smith, D.B., Cannon, W.F., Woodruff, L.G., Solano, F., and Ellefsen, K.J., 2014, Geochemical and mineralogical maps for soils of the conterminous United States: U.S. Geological Survey Open-File Report 2014–1082, 386 p., accessed August 2, 2017, at https://doi.org/10.3133/ofr20141082.

Stamos, C.L., Martin, P., Nishikawa, T., and Cox, B.F., 2001, Simulation of ground-water flow in the Mojave River basin, California: U.S. Geological Survey Water Resources-Investigations Report 2001–4002, ver. 3, 129 p., accessed November 20, 2018, at https://doi.org/10.3133/wri014002.

Stantec, 2013, Compliance with provision 1.C of cleanup and abatement order R6V-2008-0002-A4 and requirements of investigation order R6V-2013-0029: San Francisco, Calif., Pacific Gas and Electric Company, prepared by Stantec, Lafayette, Calif., [variously paged], https://geotracker.waterboards.ca.gov/esi/uploads/geo_report/8126426041/SL0607111288.pdf.

Taylor, S.R., and McLennan, S.M., 1995, The geochemical evolution of the continental crust: Reviews of Geophysics, v. 33, no. 2, p. 241–265, https://doi.org/10.1029/95RG00262.

U.S. Department of Agriculture, 1996, Soil survey laboratory methods manual: U.S. Department of Agriculture, Soil Survey Investigations Report, no. 42, version 3.0, 716 p.

U.S. Environmental Protection Agency, 2007, Method 6200—Field portable X-ray fluorescence spectrometry for the determination of elemental concentrations in soil and sediment: U.S. Environmental Protection Agency, 32 p., accessed April 13, 2020, at https://www.epa.gov/sites/production/files/2015-12/documents/6200.pdf.

U.S. Geological Survey, 2004, The National Geochemical Survey—Database and documentation: U.S. Geological Survey Open-File Report 2004–1001, accessed August 2, 2017, at https://mrdata.usgs.gov/geochem/doc/home.htm. [Also available at https://doi.org/10.3133/ofr20041001.]

U.S. Geological Survey, 2021, USGS water data for the Nation: U.S. Geological Survey National Water Information System database, accessed July 12, 2021, at https://waterdata.usgs.gov/nwis.

U.S. Geological Survey, 2022, Reference material information sheet BHVO-2 (Hawaiian Volcano Observatory Basalt), 3 p., accessed October 31, 2022 at https://d9-wret.s3.us-west-2.amazonaws.com/assets/palladium/production/s3fs-public/media/files/USGS-BHVO-2-IS_2022-508.pdf.

Wold, S., Esbensen, K., and Geladi, P., 1987, Principal component analysis: Chemometrics and Intelligent Laboratory Systems, v. 2, no. 1–3, p. 37–52, https://doi.org/10.1016/0169-7439(87)80084-9.

For more information concerning the research in this report, contact the

Director, California Water Science Center
U.S. Geological Survey
6000 J Street, Placer Hall
Sacramento, California 95819
https://ca.water.usgs.gov

Publishing support provided by the U.S. Geological Survey
Science Publishing Network, Sacramento Publishing Service Center

Izbicki and Groover—**Chapter B: Survey of chromium and selected element concentrations in rock, alluvium, and core material**—PP 1885-B

ISSN 2330-7102 (online)
https://doi.org/10.3133/pp1885B